AD-A125 790 CONVERSION OF A CYLINDRICALLY CONFINED SURFACE EXPLOSION INTO A ONE-DIMENSIONAL BLAST WAVE(U) NAVAL RESEARCH LAB WASHINGTON DC M A FRY ET AL. 24 FEB 83 1/1

UNCLASSIFIED NRL-MR-5021 F/G 18/3 NL

END
DATE
FILMED
4-83
DTIC

M-2

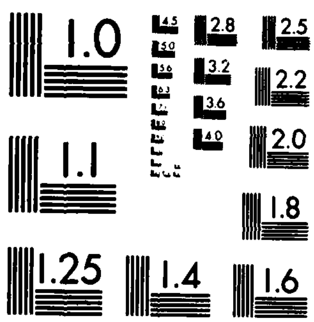

MICROCOPY RESOLUTION TEST CHART
NATIONAL BUREAU OF STANDARDS 1963 A

AD A125790

GRID

SECURITY CLASSIFICATION OF THIS PAGE (When Data Entered)

REPORT DOCUMENTATION PAGE		READ INSTRUCTIONS BEFORE COMPLETING FORM
1. REPORT NUMBER NRL Memorandum Report 5021	2. GOVT ACCESSION NO. AD-A125790	3. RECIPIENT'S CATALOG NUMBER
4. TITLE (and Subtitle) CONVERSION OF A CYLINDRICALLY CONFINED SURFACE EXPLOSION INTO A ONE-DIMENSIONAL BLAST WAVE		5. TYPE OF REPORT & PERIOD COVERED Interim report on a continuing NRL problem. 6. PERFORMING ORG. REPORT NUMBER
7. AUTHOR(s) M. A. Fry* and D. L. Book		8. CONTRACT OR GRANT NUMBER(s)
9. PERFORMING ORGANIZATION NAME AND ADDRESS Naval Research Laboratory Washington, DC 20375		10. PROGRAM ELEMENT, PROJECT, TASK AREA & WORK UNIT NUMBERS 62715H; 44-0578-03
11. CONTROLLING OFFICE NAME AND ADDRESS Defense Nuclear Agency Washington, DC 20305		12. REPORT DATE February 24, 1983 13. NUMBER OF PAGES 64
14. MONITORING AGENCY NAME & ADDRESS(if different from Controlling Office)		15. SECURITY CLASS. (of this report) UNCLASSIFIED 15a. DECLASSIFICATION/DOWNGRADING SCHEDULE

16. DISTRIBUTION STATEMENT (of this Report)

Approved for public release; distribution unlimited.

17. DISTRIBUTION STATEMENT (of the abstract entered in Block 20, if different from Report)

18. SUPPLEMENTARY NOTES

*Present address: Science Applications, Inc., McLean, VA 22102.
This work was supported by the Defense Nuclear Agency under Subtask Y99QAXSG, work unit 00027, and work unit title "Flux-Corrected Transport Code."

19. KEY WORDS (Continue on reverse side if necessary and identify by block number)

Blast waves	Basing modes
Explosion	Close-spaced basing
Mach reflection	
Adaptive gridding	

20. ABSTRACT (Continue on reverse side if necessary and identify by block number)

The NRL Flux-Corrected Transport code FAST2D is used to model the conversion of a cylindrically confined surface explosion into a one-dimensional blast wave. The ideal gasdynamic equations are used, together with a real-air equation of state, to follow the development of an explosion initialized with the 1-kton standard as it reflects from the cylindrical boundary and propagates upward. Multiple shocks develop and the solution quickly (in 1-2 reflection times) approaches the one-dimensional asymptotic state described by the Taylor-Sedov similarity solution.

DD FORM 1 JAN 73 1473 EDITION OF 1 NOV 65 IS OBSOLETE
S/N 0102-014-6601

SECURITY CLASSIFICATION OF THIS PAGE (When Data Entered)

CONTENTS

CONVERSION OF A CYLINDRICALLY CONFINED SURFACE EXPLOSION INTO A ONE-DIMENSIONAL BLAST WAVE

I. INTRODUCTION

In connection with the Dense Pack (Close-Spaced Basing) scheme, it has been pointed out by Latter that surface environments following a multiburst attack could be considerably more difficult to survive than those resulting from single bursts. Detonation simultaneously over all the shelters of a closely spaced array surrounds the vicinity of an individual shelter with high pressures, allowing the explosion to vent only in the upward direction. Hence, at least in the interior of the array, extremely high pressures are maintained for longer times, with the result that total impulses applied to ground structures are much greater than for a solitary explosion.

Latter proposed considering the following idealized situation: identical explosions are initiated simultaneously in an infinite regular hexagonal array at (or near) a uniform level plane surface (Fig. 1). Construct a vertical plane transverse to the line connecting every pair of neighboring centers, at the midpoint of the line. By symmetry, the six planes surrounding an explosion represent perfectly reflecting surfaces and together form a hexagonal parallelepiped (a cylinder having hexagonal cross section) with a vertical axis. This in turn can be approximated as a right circular cylinder with the same axis and cross sectional area. A two-dimensional r-z code can be used to solve this idealized problem for surface and air bursts. It is clear, however, that asymptotically the flow becomes one-dimensional, evolving into a shock tube solution. In the limit where this asymptotic state has been

Manuscript approved November 9, 1982.

reached and where many weapon masses of air have been swept over, the one-dimensional form of the Sedov point blast solution should apply. The pressure on the ground as a function of time t is given by

$$p = k\ \rho_o \frac{W}{\rho_o A t}^{2/3}, \tag{1}$$

where ρ_o is the air density, W is the weapon yield, A is the cylinder area, and k is the function of the adiabatic index γ which is $\lesssim 1$. This is to be compared with the corresponding result for the case of a spherical free-field expansion, which is of the form

$$p = k' \rho_o \left(\frac{W}{\rho_o t^3}\right)^{2/5} . \tag{2}$$

As may be seen, the pressure given by Eq. (1) decreases in time more slowly than that of Eq. (2). Although the idea behind this so-called "bomb-in-a-can" model is simple and transparent, it leaves several important questions unanswered. First, how long (how many shock reflections) does it take to reach the asymptotic state, i.e., when does Eq. (1) become a good approximation? Second, to what extent is the prediction (1) dependent on idealizations of the model, e.g., perfect symmetry, perfect simultaneity, neglect of scouring and entraining of dust, etc? Finally, what are the long-term tactical consequences in this model of a multiburst scenario--specifically, what can be said about the shape of the plume produced, how much dust is raised up and where does it go, what sort of turbulence is established and what are the consequences for radar transmission, etc?

In this report we describe a calculation which was carried out to investigate the first question, regarding the approach to the one-dimensional solution. We have used a version of the DNA one kiloton (1-kton) standard to

initialize a surface burst equivalent to 18 scaled megatons (Mton) in a cylinder of radius 900 feet. We find that the flow is close to one-dimensional after ~20 ms (the time required for the blast to reflect from the cylindrical wall and return to the origin, considerably less than might have been expected.

In the following section we describe in detail the calculations and the results obtained, and conclude with a brief discussion of what we intend to do in follow-on work.

2. TWO DIMENSIONAL CALCULATION

The development of the explosion can be viewed in terms of four stages. These are (1) the spherical free-field expansion prior to reflection at the outer boundary; (2) multiple distinct reflections off both boundaries, during which the transition to one-dimensional flow takes place; (3) approximately one dimensional expansion after reflecting gas-dynamic discontinuities are no longer discernible; (4) a gradual transition to three-dimensional flow as the finite extent of the array communicates itself to the interior. Stage (1) is not contained in our model; since the weapon mass greatly exceeds the mass of air contained within the initial explosion radius, the nature of the weapon and its constituents ought to be important in this stage, but no attempt has been made to improve on the realism of the 1-kton standard. Likewise, stage (4) is absent from the model (but see remarks in our concluding section below). Instead, we attempted to model stages (2) and (3).

The calculation was performed with 100 zones, each 10.2 cm in width in the radial direction, and 100 zones in the axial direction, 90 of which were 20.4 cm in length and the final 10 of which geometrically increased by increments of 11% (Fig. 2a). The final grid size was 10.2 m by 22.4 m. An equivalent 18 Mton surface burst was achieved by inserting values of density, energy, and momentum scaled from the 1 kton standard. Since values of the 1 kton standard were only available from 10 meters (an 18 Mton surface burst scales to about eight meters after we double the yield to account for surface reflection), we created initial profiles by increasing the density, internal energy, and momentum by a factor of 1.4. As a result the initial energy was

3.1×10^{19} ergs and the mass was 8.2×10^6 g, deposited into a hemisphere of 10 m radius. The effect of this scaling was to simulate the initiation of an event with the appropriate yield and weapon mass, but with profiles (as a function of distance from the burst site) which were not correct in detail. During the early phases of the problem they must give rise to discrepant behavior, but at later times this presumably becomes insignificant.

The numerical simulation was performed using the NRL FAST2D code which utilizes the latest version of Flux Corrected Transport (FCT). The code was essentially the same configuration used previously for 104-ft and 50-ft 1-kton HOB calculations. A reflection condition was imposed on the left and bottom boundaries, as before, and on the right-hand boundary as well. In addition to the diagnostics employed previously, we introduced several devised specifically for this problem.

Figure 2b shows plots of the initial profiles of the mass density, velocity, pressure and energy density. Note that all of these variables achieve their maxima at the leading shock. To convert these profiles into their counterparts for the 18 Mton case, it is necessary to dilate by a factor of $(900 \text{ ft}/10 \text{ m})^{1/3} = 27.4$. Likewise, the time scale has to be expanded by the same factor.

The reflection of this initial blast wave from the outer radius of the can and the subsequent evolution of the system are depicted in Fig. 3. This shows pressure contours and velocity vectors plotted at intervals of 100 cycles (approximately 30-50 μs). Although the time intervals vary because of the changing time step, these plots are in a sense equally separated in terms of the "total change" in the system, because when flow and sound speeds are

large the timestep decreases, and vice versa. Note how rapidly the reflected shock propagates to the left; almost invisible at cycle 201, it is nearly halfway across the mesh at cycle 301. It travels upward almost as rapidly, reaching an altitude of 10 m by cycle 601. By cycle 801 it appears to have overtaken the primary shock wave, which is considerably distorted after cycle 1501. On the right hand boundary the reflection, which is initially regular, gradually converts to Mach reflection. This development is of course analogous to the transition to Mach reflection observed in the HOB case[3]. It is hard to see exactly when transition occurs, but a Mach stem is clearly visible in the pressure plots at cycle (40) and thereafter. If we examine Carpenter's results regarding the boundary between regular and Mach reflection in real air at Mach numbers $M \gtrsim 10$, we see that the angle at which transition occurs depends on M only weakly and is approximately equal to 45^0. The Mach stem ought thus to have first formed around cycle 701 to 801, but the region of reflection is not sufficiently well resolved to show it.

In Fig. 4 another view of the same time sequence is shown. These surface pressure plots are particularly well suited for showing shock and rarefaction waves propagating through the sytem. Since the pressures are interpolated onto a regular mesh before plotting, peak values are lowered by as much as a factor of two. This reduces contrast somewhat and makes some features appear to move up and down erratically in time, but the overall morphology is very clear. We see, for example, how the shock reflected radially from the origin appears to run out of gas at about cycle 901, while a train of waves reverberates down from the top. One of these finally reaches the radially-propagated ground shock at about cycle 1801 and begins to push it along. Throughout this time the pressures in the lower right corner of the system

remain low. Meanwhile, the shock front rising toward the top of the system, which is madly churning around at cycle 1201, becomes smoother as shocks propagate back down from it.

Figure 5 shows the pressure recorded at a series of sensors located across the bottom of the can, ranging from the burst center (a) to the outer edge (ℓ). Note that, although the initial profiles have a sharp (one-zone) discontinuity at the leading edge, the pressure peak at sensor ℓ takes about 70 μs to build up to the maximum. This is about a hundred times as long as it takes the shock to propagate across one zone. It is, however, not out of line with the time required for the air behind the shock (velocity 1.5×10^6 cm/s) to cross a zone, about 7 μs. The density (and other fluid variables) can build up to their post-reflection values when the air from $(\gamma+1)/(\gamma-1) \approx 10$ cells has been compressed into the cell closest to the wall. Using Carpenter's[4] reflection factors for normally incident shocks, we calculate that the free-field pressure, initially 3.5 kbar, should reflect up to about 40 kbar, which is to be compared with the value of 25 kbar we actually obtained. If we look at sensors closer to the burst site, we see that the pressure peaks get continuously sharper, finally turning into an almost discontinuous spike at the origin, as the imploding shock attempts to develop into a singularity.

The information in these pressure histories is capsulized in Fig. 6, which shows the maximum pressure recorded during the course of the calculation as a function of sensor location. Note that the peak at $r = 0$ is nearly as high as that at the periphery, in contrast with results reported by Pyatt[5]. This may be attributable to the lower resolution he used, or to the greater numerical dissipation in the HULL code. Only one peak was detected at each

sensor location. Our calculation was run for less than 1 ms, or (scaled to 18 Mton) rather less than the 30 ms Pyatt required to see a second peak at the periphery when the re-reflected shock impinges there; the two calculations are thus not inconsistent in this regard.

The approach to one-dimensional motion may be inferred from the contour plots of Fig. 4, where it is seen that the leading edge of the upward-propagating blast wave becomes more and more horizontal, and from the velocity vector plots of Fig. 3, which show that the flow becomes increasingly vertical and that velocities well behind the upper front tend to die away. A more quantitative comparison is possible if we compute the average pressure on the bottom,

$$\bar{p} = \frac{2\pi \int_0^R p(r,0)rdr}{2\pi \int_0^R rdr} \tag{3}$$

as a function of time. The result is shown as the solid line in Fig. 7. For comparison, formula (1) has been added (broken line), using yield $W = 1.4$ kton and area $A = 100\pi\ m^2$, with $\gamma = 1.2$. The agreement between the two is striking, particularly since we expect to observe it only asymptotically. It is clear that the one-dimensional approximation becomes valid very early, probably because the reverberating shocks behind the leading front of the blast propagate so rapidly in the hot medium.

3. CONCLUSIONS

We have successfully modelled the "bomb-in-a can" using FAST2D, a general-purpose code which required no special modification for this problem. Although we only ran the calculation out to an altitude of about 20 m (twice the system radius), the sliding grid (continuous adaptive rezone) capability of FAST2D allows us to continue the run as long as desired by stretching the mesh in the vertical direction.

Our results show that the asymptotic one-dimensional state is approached very rapidly, apparently because the multiply reflected shocks propagate much faster than the original blast wave. Two or three reflections across the radius of the system effectively equilibrate the flow and relax it to a state of vertical expansion. The simulation reveals a complex pattern of reverberations, with reflection occurring off all the boundaries and regions where conditions are highly nonuniform.

A number of modifications are required to make these results applicable to an actual tactical situation. Perhaps the most important is the inclusion of dust scoured up from the ground and entrained in the wind fields following the blast. A realistic description would require not only that the dust mass load the air, but that air and dust be permitted to exchange momentum and energy. The bottom boundary conditions should also be changed to model the energy that goes into cratering and scouring.

If the calculation is to be continued to late times, atmospheric stratification should be included. The effects of water vapor and turbulence

should also be modelled. Also, venting of the explosion in the horizontal direction (in the case of an RV exploding near the edge of a finite-sized array of shelters, or for an explosion in the interior of the array which has begun to feel the pressure in the outer explosions drop as they vent outward) can be modelled by having the radius R increase as a function of height. Of course, airblast situations in which the explosion originates above the ground can also be investigated (in which case Mach stems could appear on the ground as well as the sides of the system).

Although some of these extensions require nontrivial code modifications, there is no reason in principal why the present results could not be augmented and refined greatly by additional calculations.

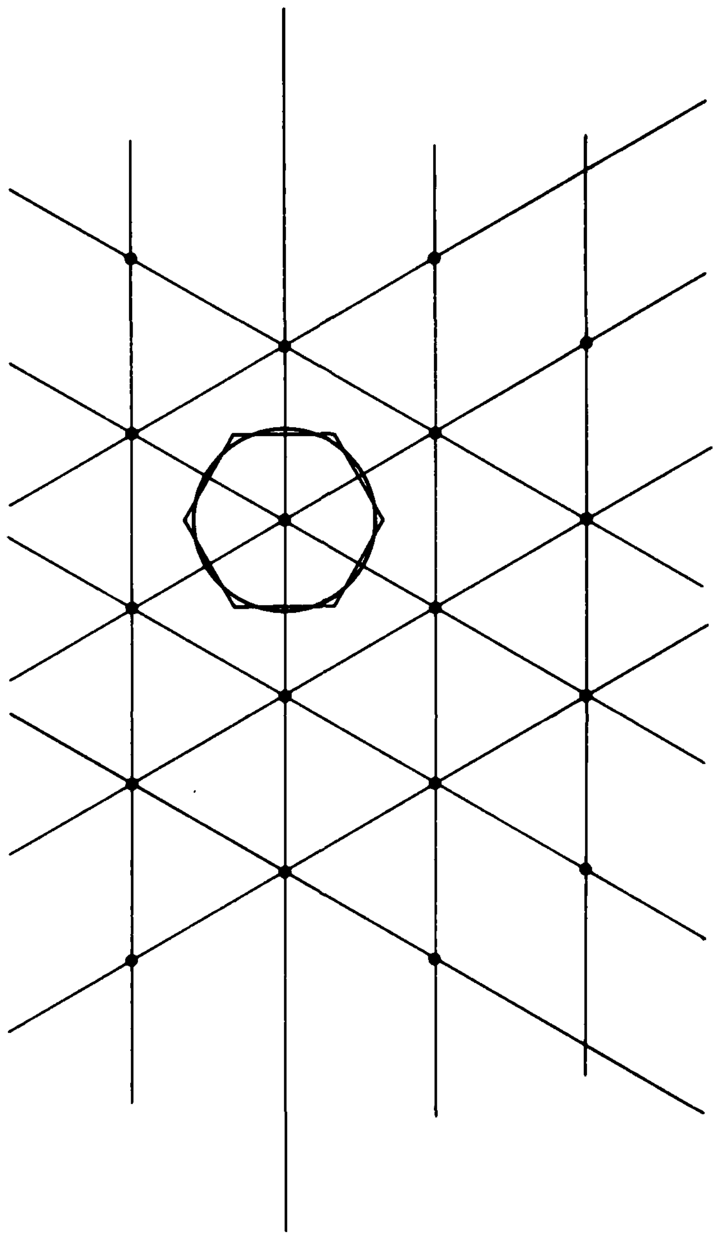

Fig. 1 — Schematic of unbounded hexagonal array of shelters with 1800 ft separations on a perfectly reflecting plane. Shown is the cross section of the hexagonal parallelpiped formed by the planes bisecting the lines connecting a given shelter with its six nearest neighbors (reflection planes), along with the coaxial cylinder having the same cross sectional area.

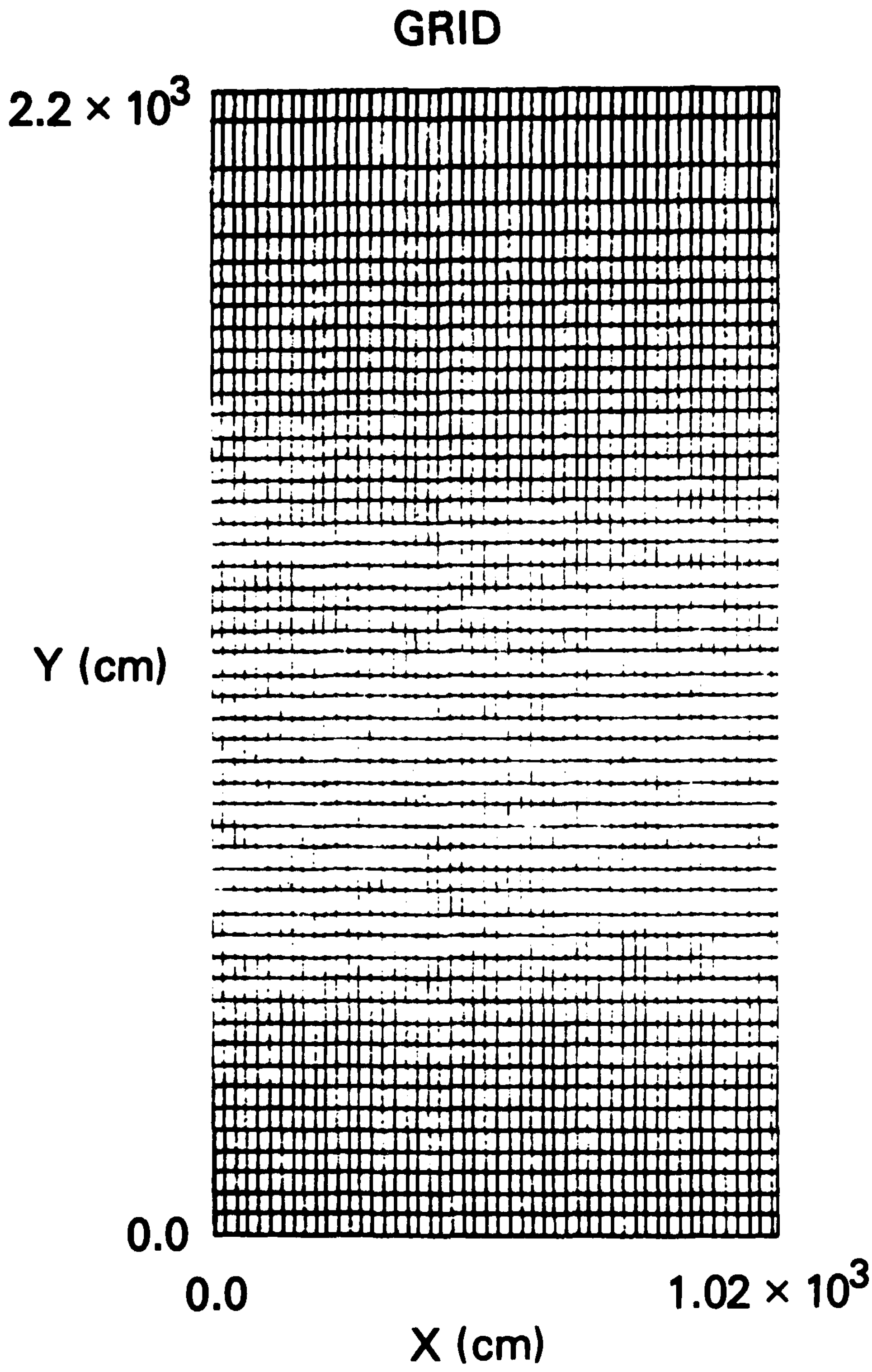

Fig. 2(a) — Mesh used in the calculation. Zones are of equal width in the radial direction, but are stretched vertically near the top of the mesh.

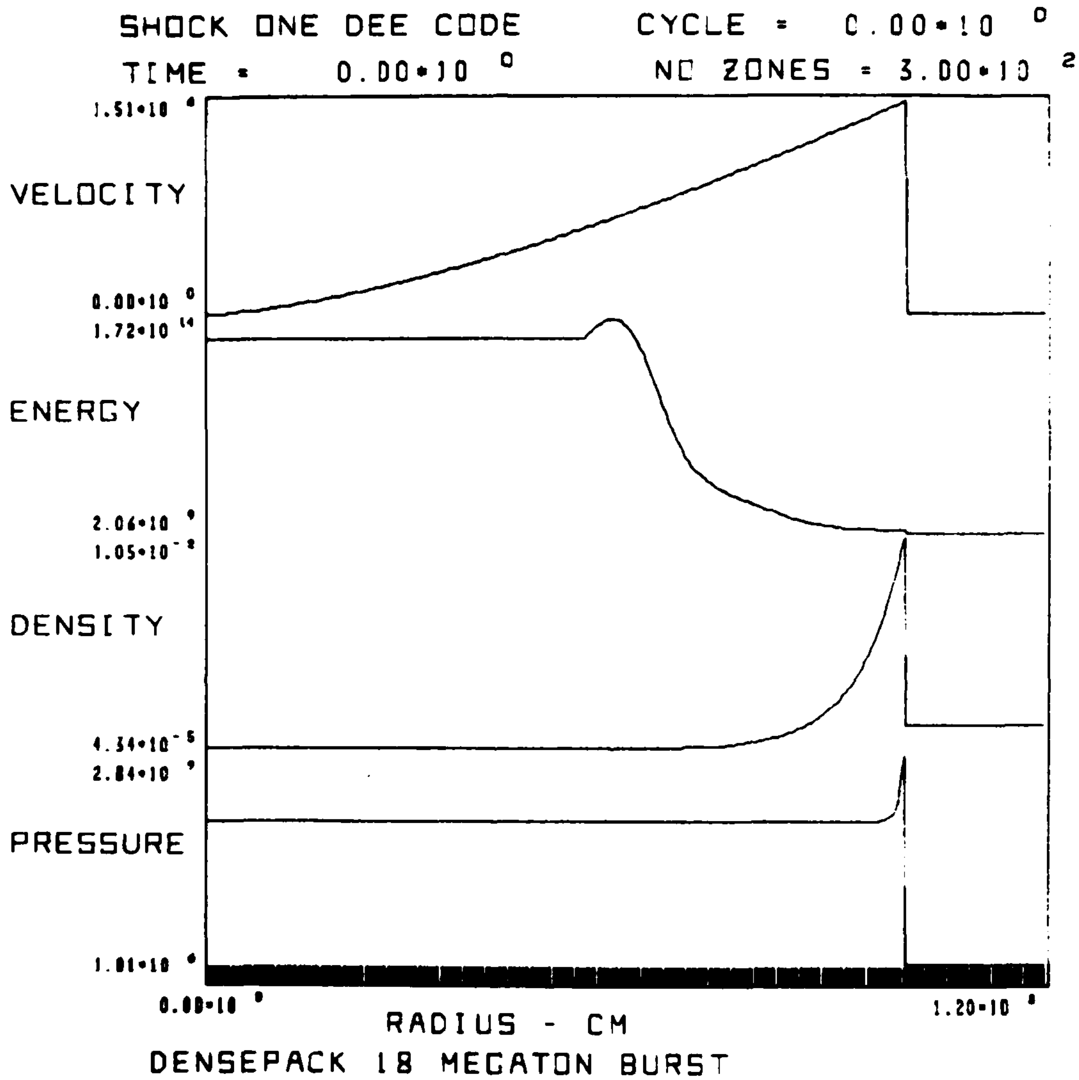

Fig. 2(b) — Profiles used to initialize calculations (modification of the 1-kton standard). Velocities are directed radially outward from burst site at origin.

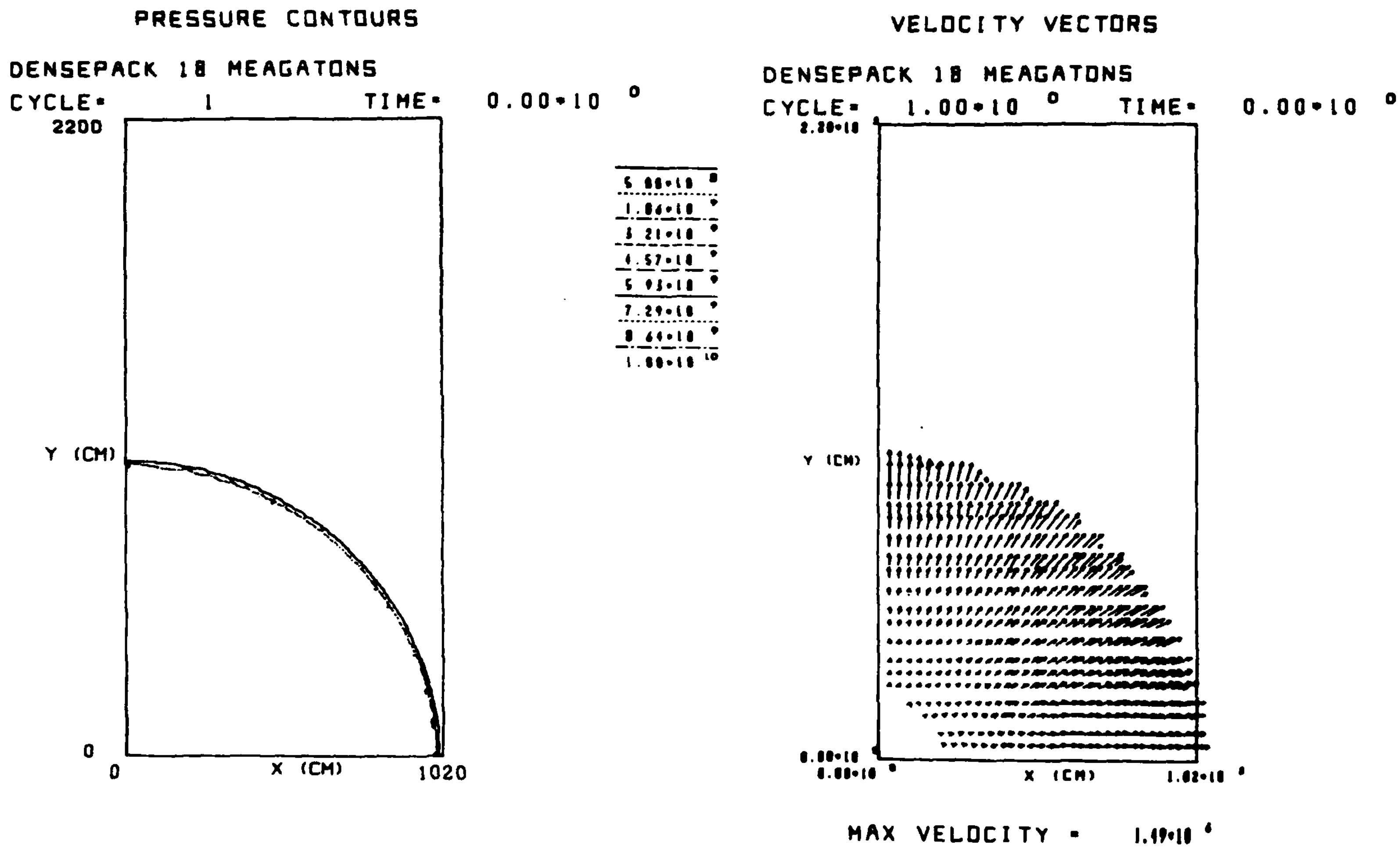

Fig. 3a — Pressure contours and velocity vectors calculated using FAST2D, shown at intervals of 100 cycles

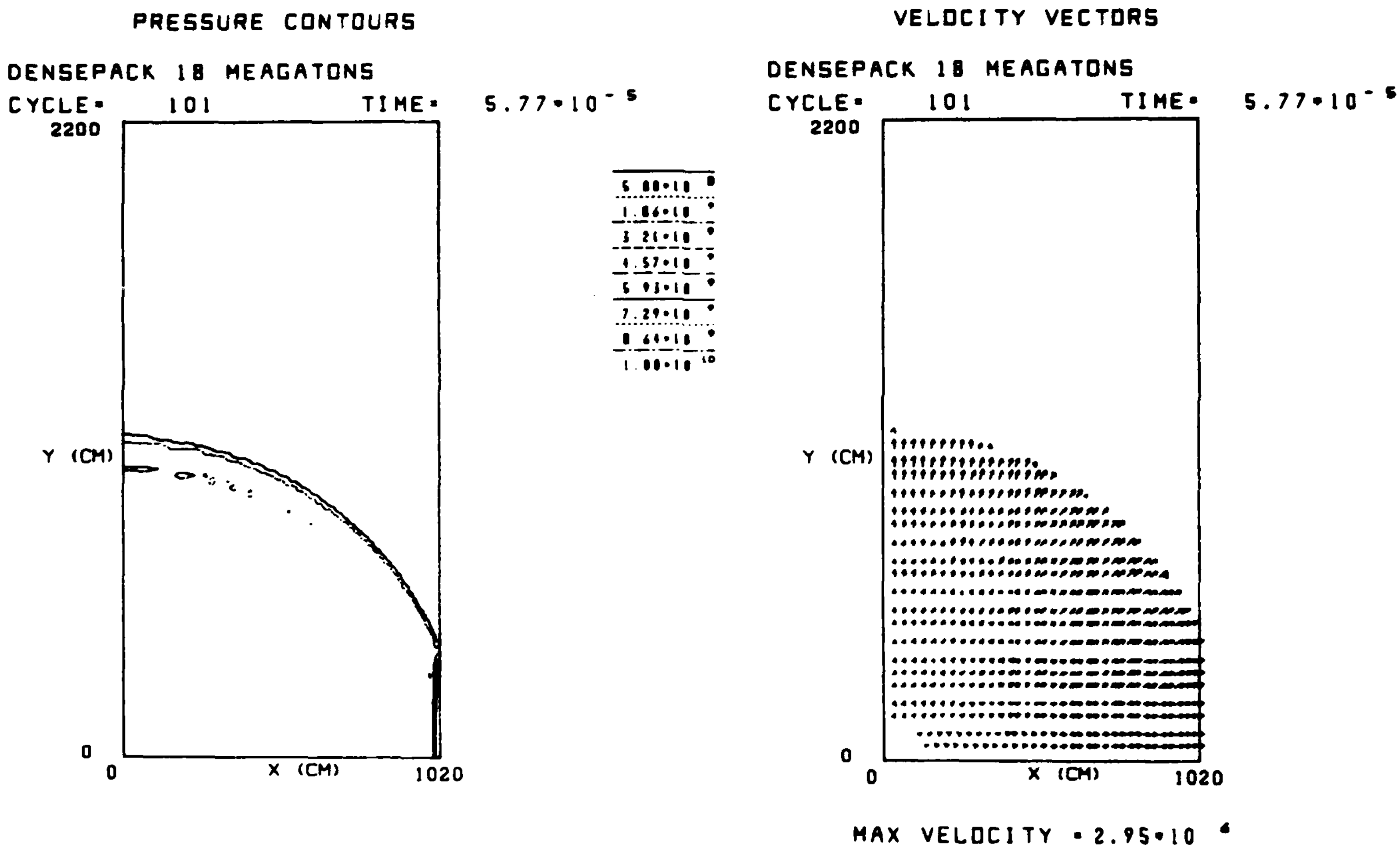

Fig. 3b — Pressure contours and velocity vectors calculated using FAST2D, shown at intervals of 100 cycles

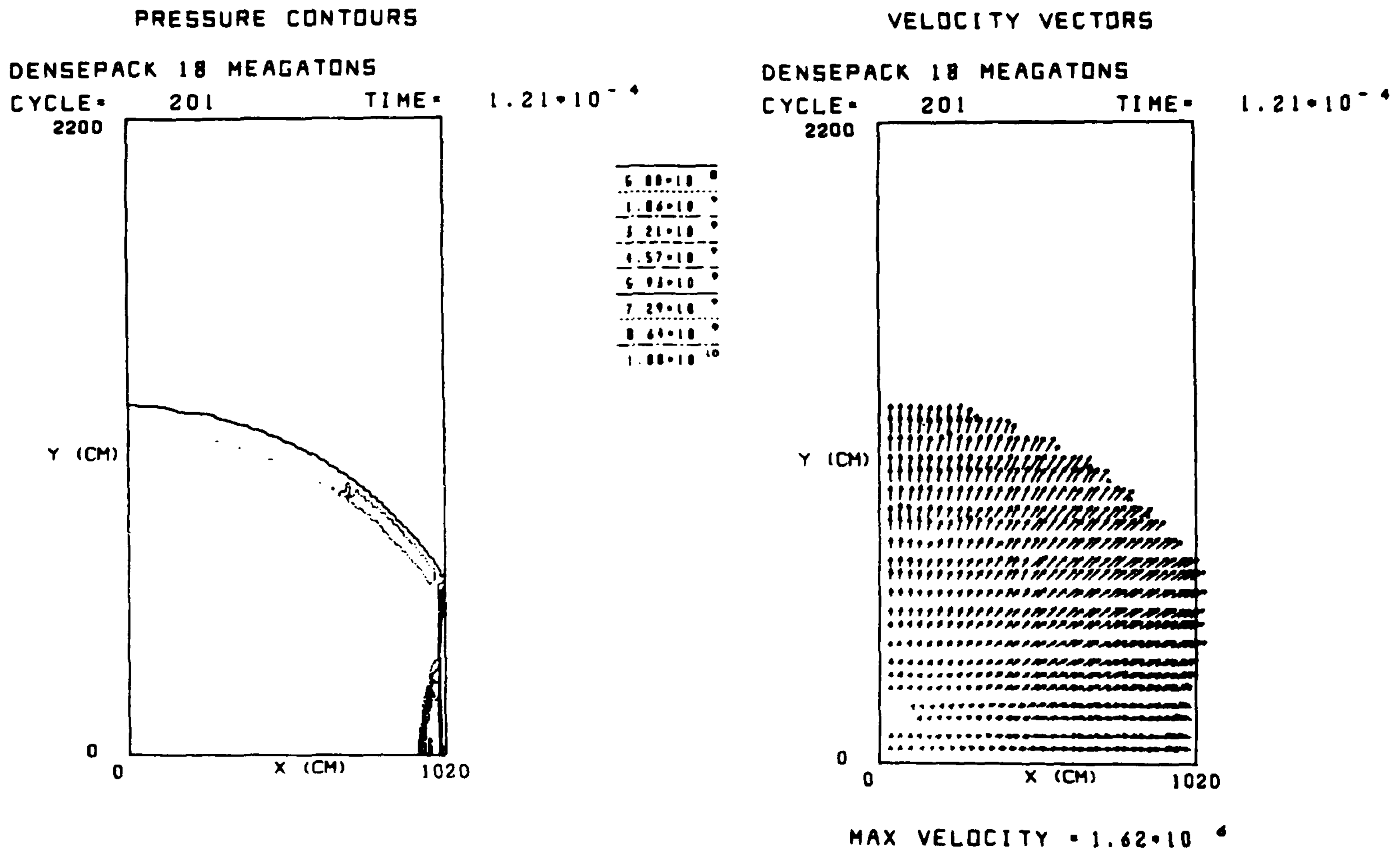

Fig. 3c — Pressure contours and velocity vectors calculated using FAST2D, shown at intervals of 100 cycles

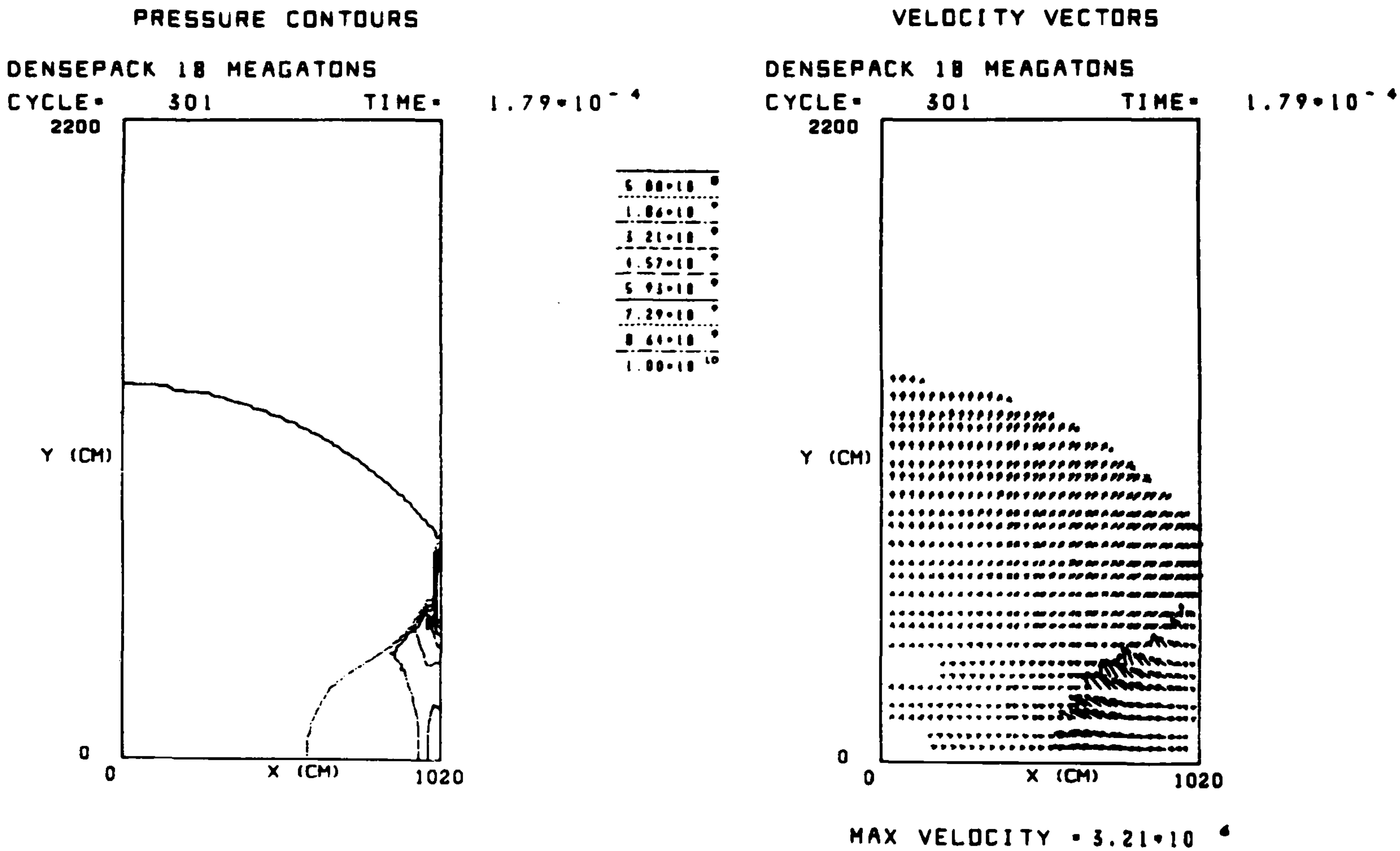

Fig. 3d — Pressure contours and velocity vectors calculated using FAST2D, shown at intervals of 100 cycles

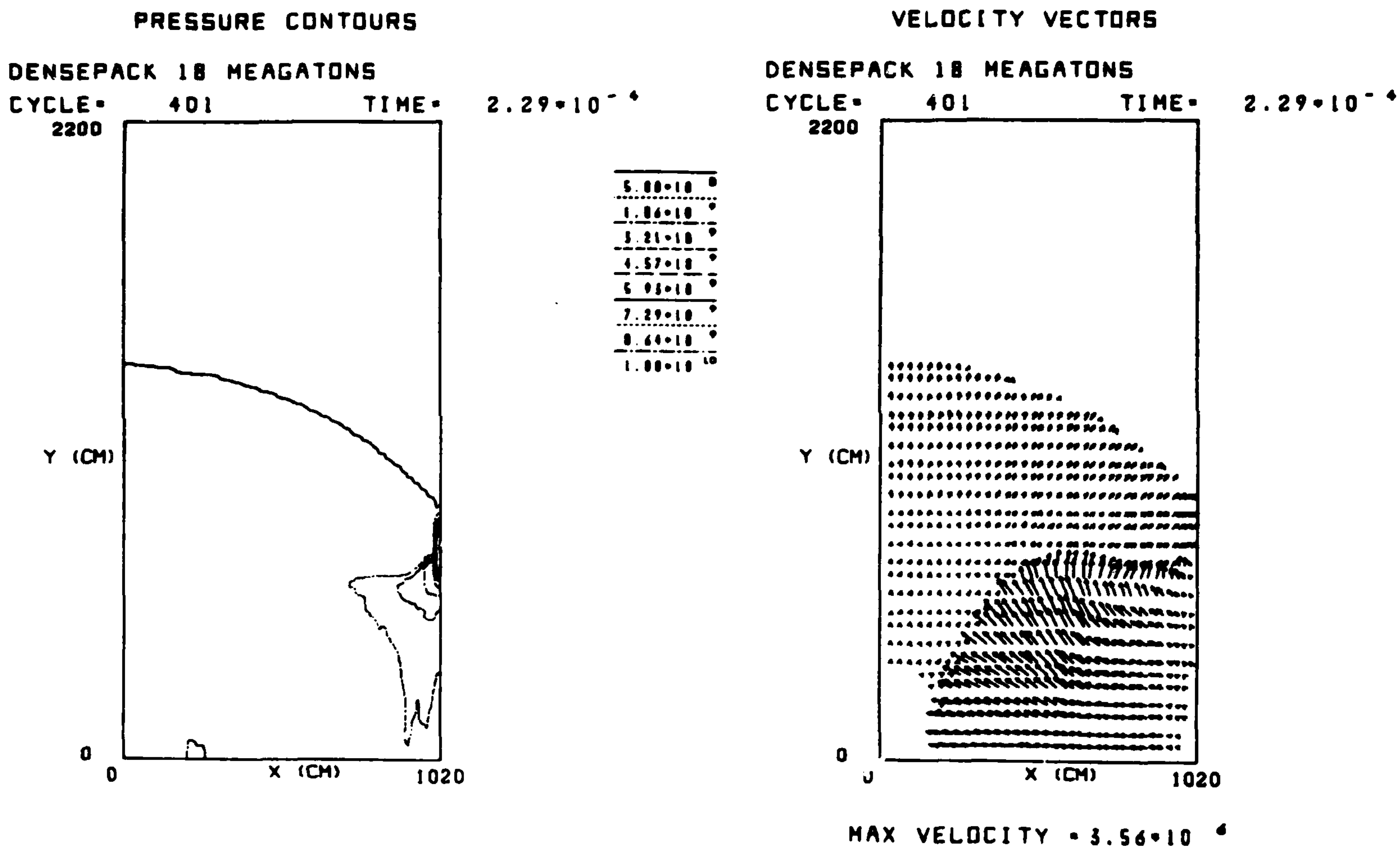

Fig. 3e — Pressure contours and velocity vectors calculated using FAST2D, shown at intervals of 100 cycles

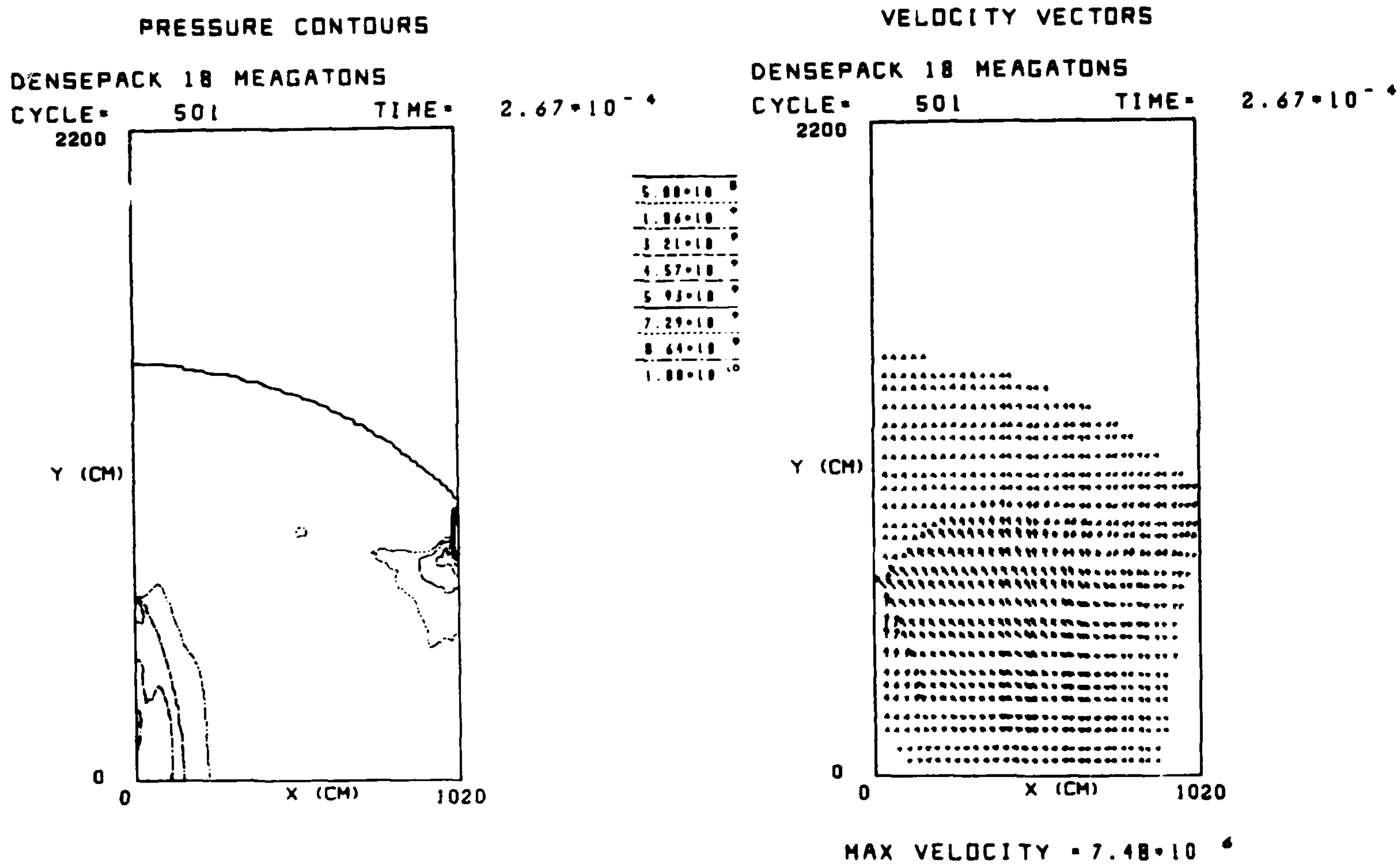

Fig. 3f — Pressure contours and velocity vectors calculated using FAST2D, shown at intervals of 100 cycles

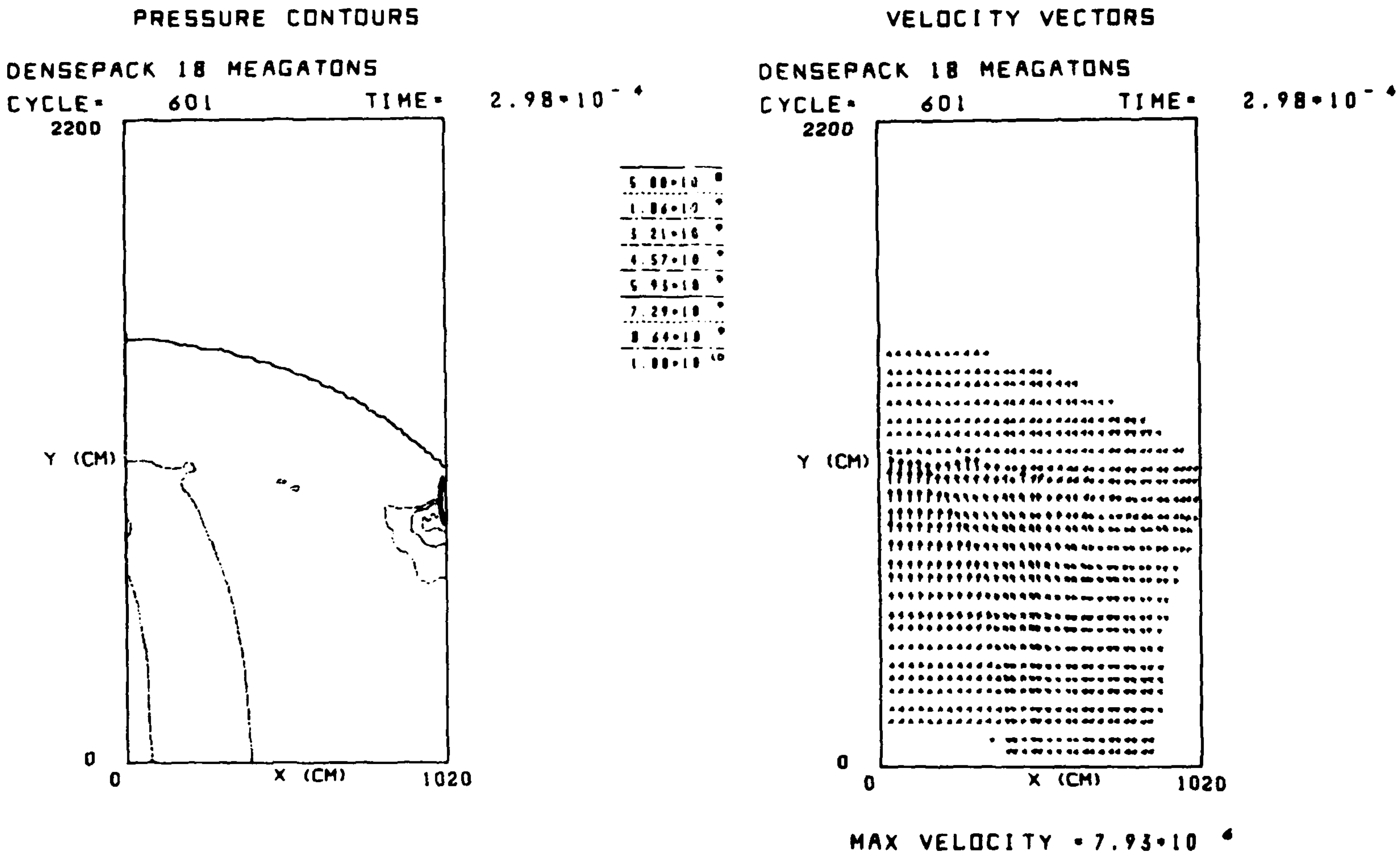

Fig. 3g — Pressure contours and velocity vectors calculated using FAST2D, shown at intervals of 100 cycles

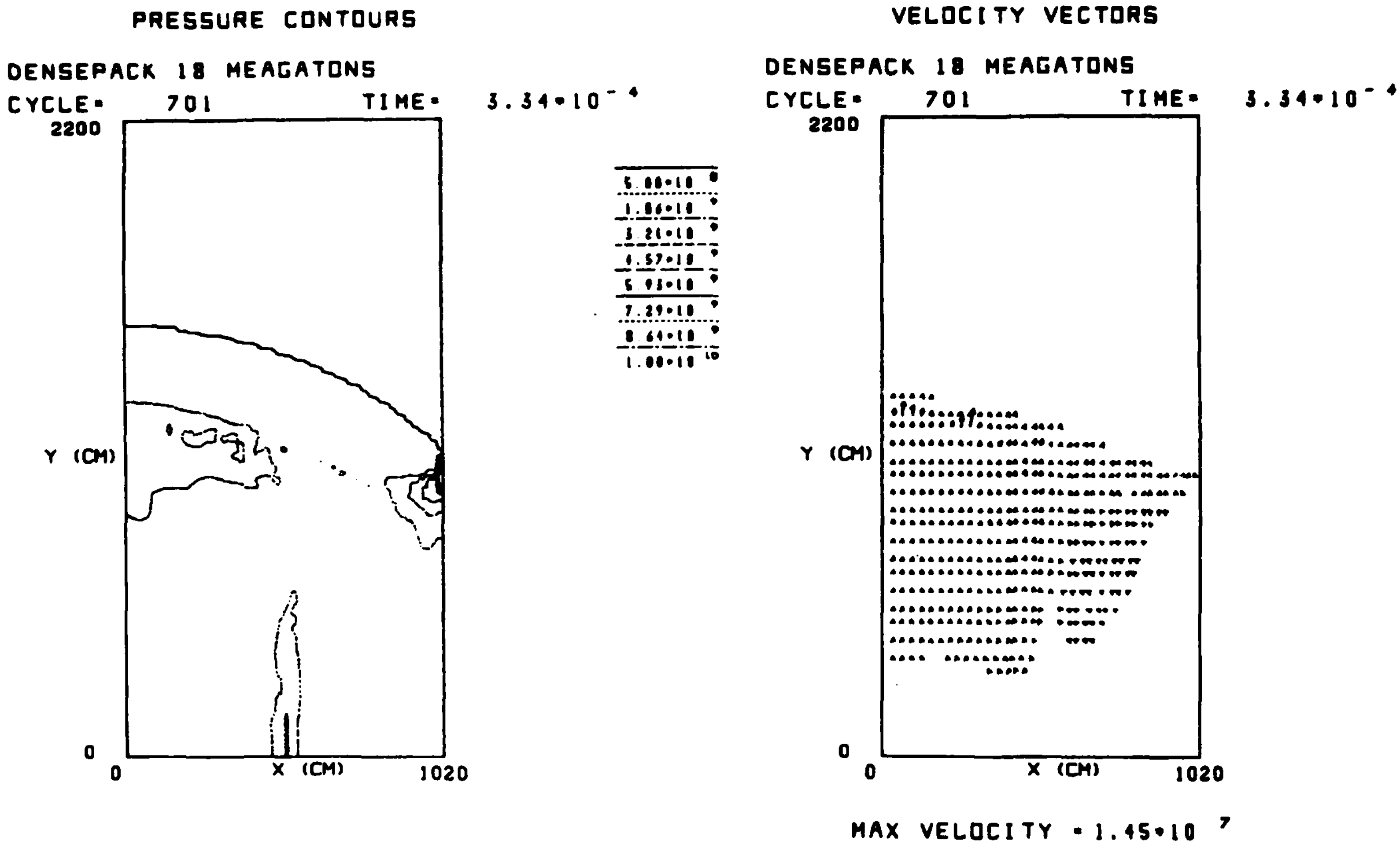

Fig. 3h — Pressure contours and velocity vectors calculated using FAST2D, shown at intervals of 100 cycles

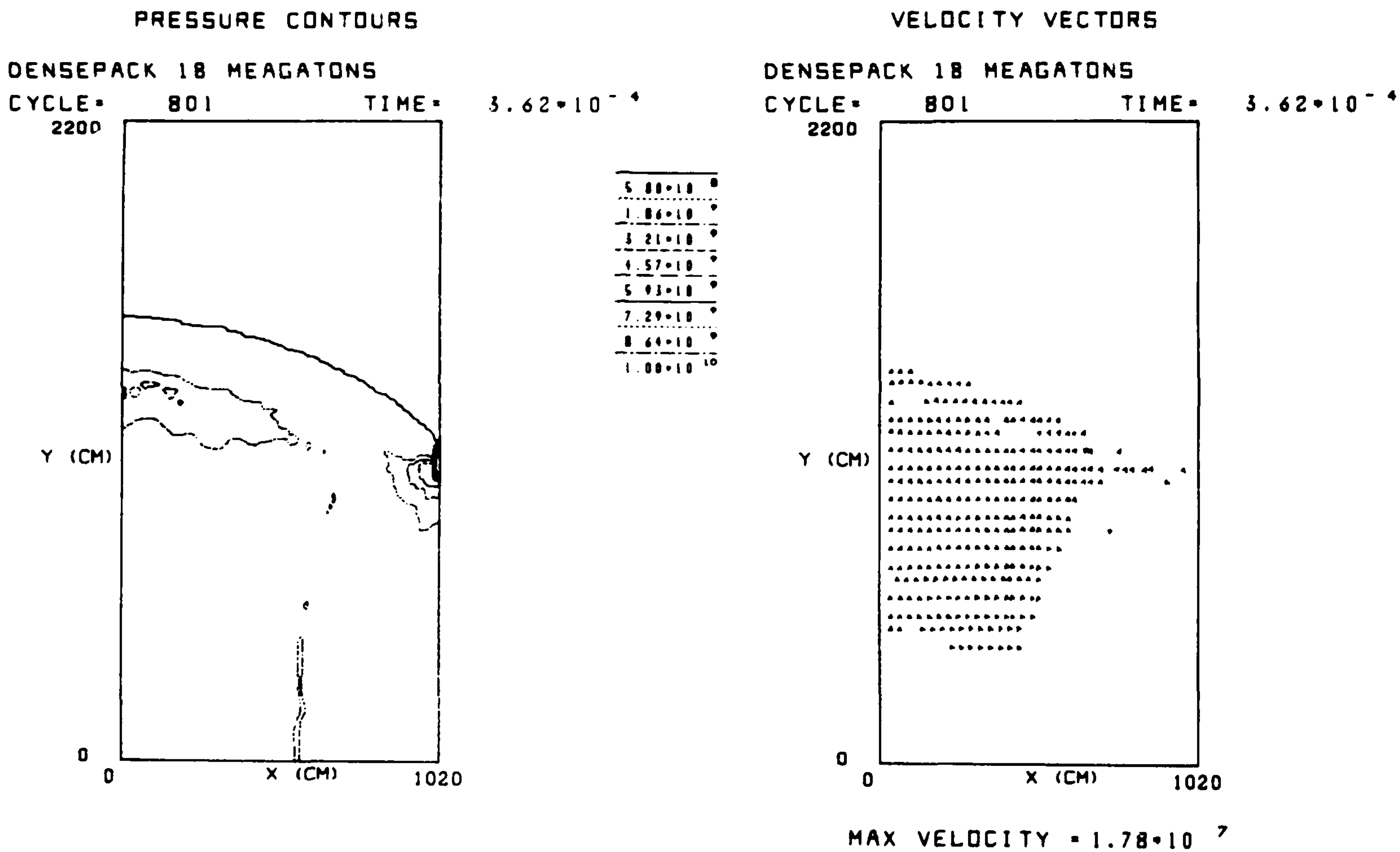

Fig. 3i — Pressure contours and velocity vectors calculated using FAST2D, shown at intervals of 100 cycles

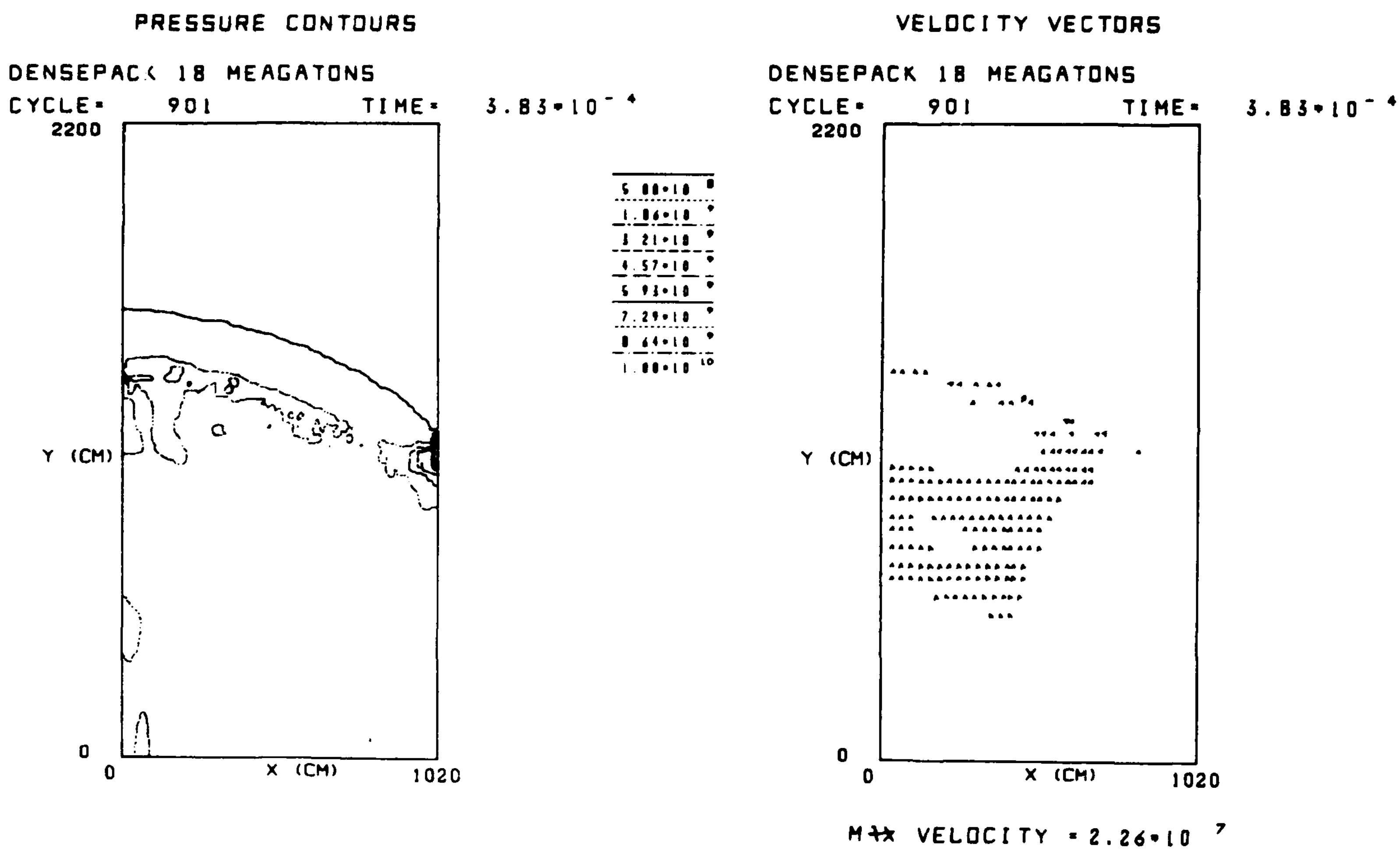

Fig. 3j — Pressure contours and velocity vectors calculated using FAST2D, shown at intervals of 100 cycles

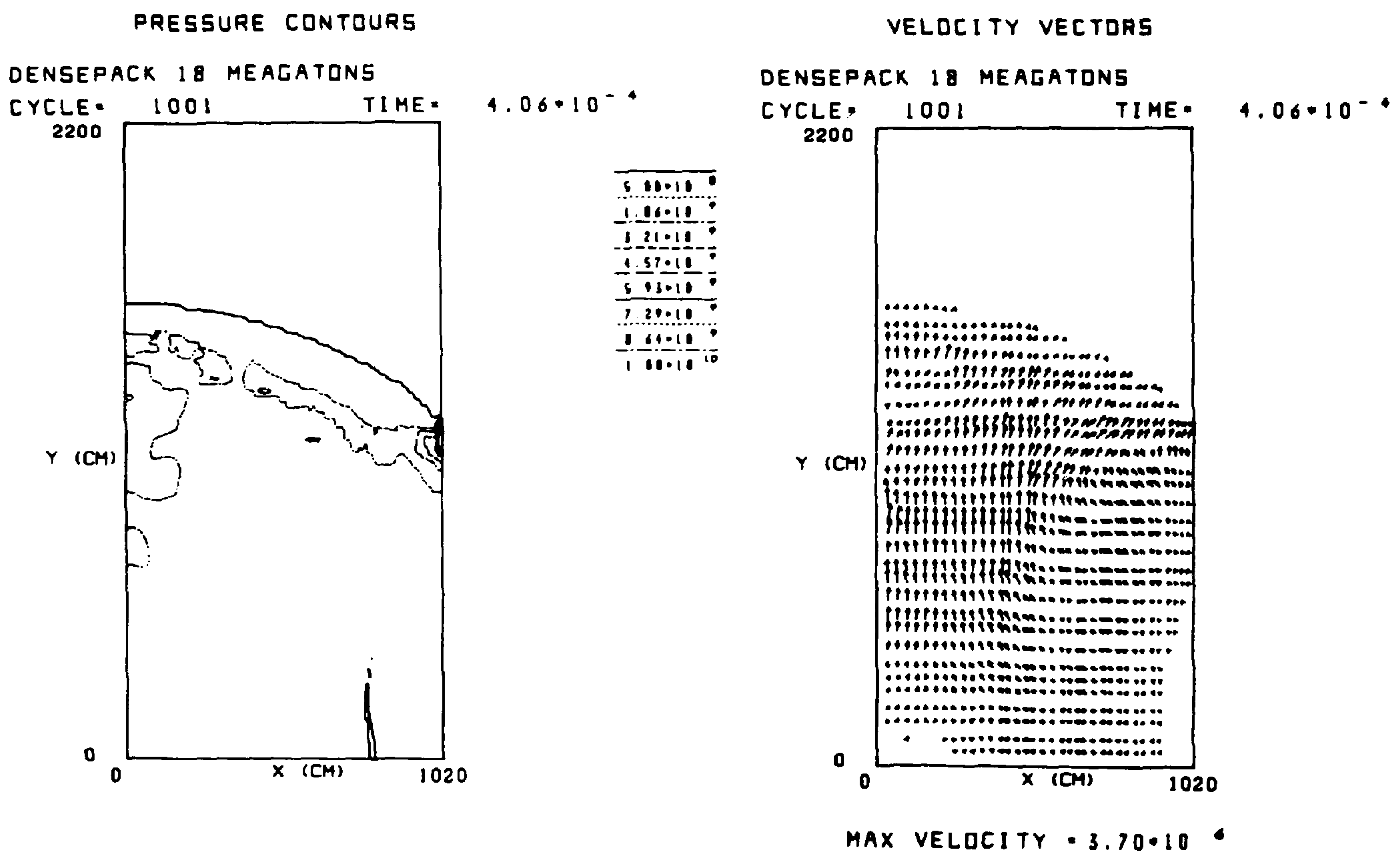

Fig. 3k — Pressure contours and velocity vectors calculated using FAST2D, shown at intervals of 100 cycles

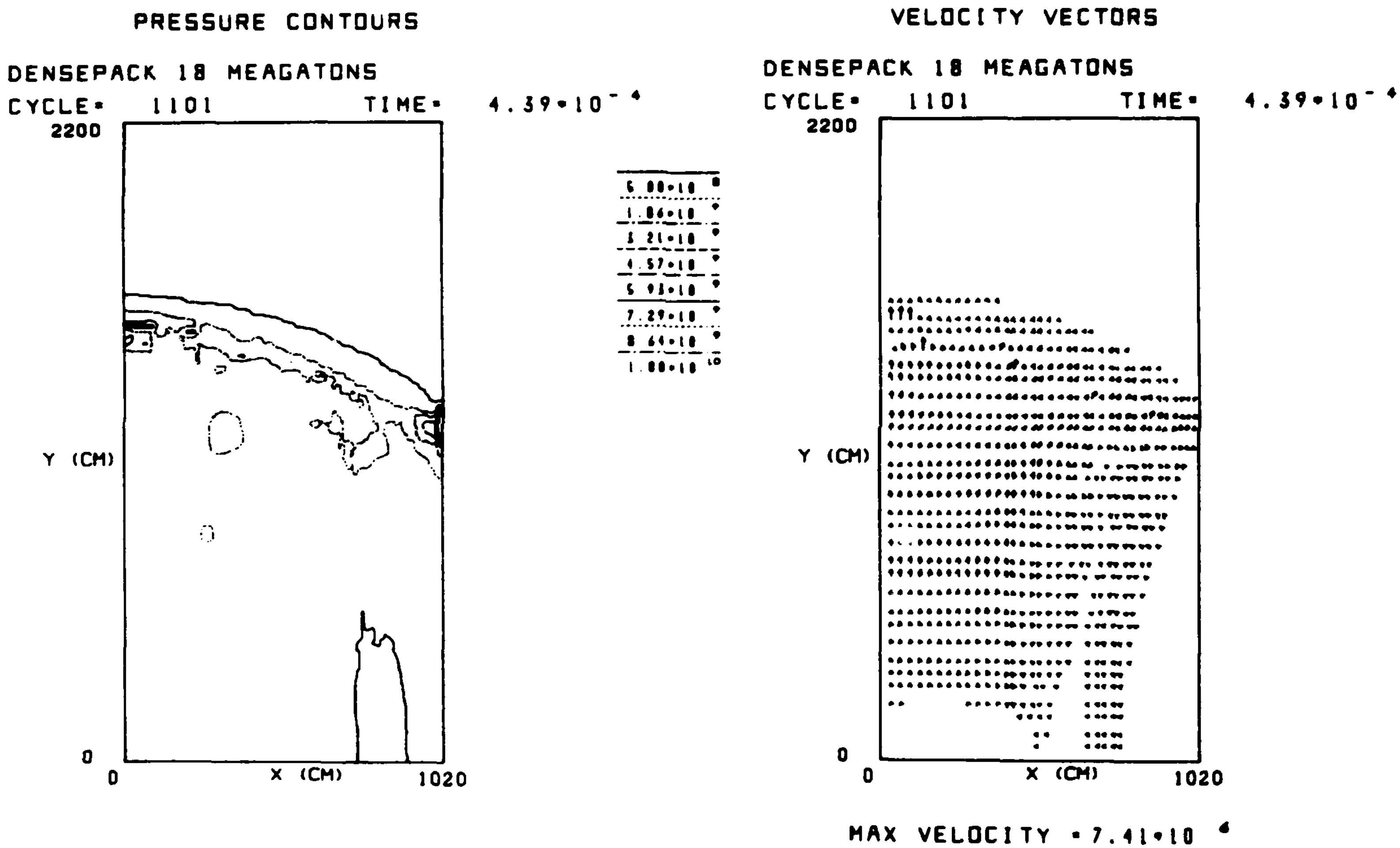

Fig. 31 — Pressure contours and velocity vectors calculated using FAST2D, shown at intervals of 100 cycles

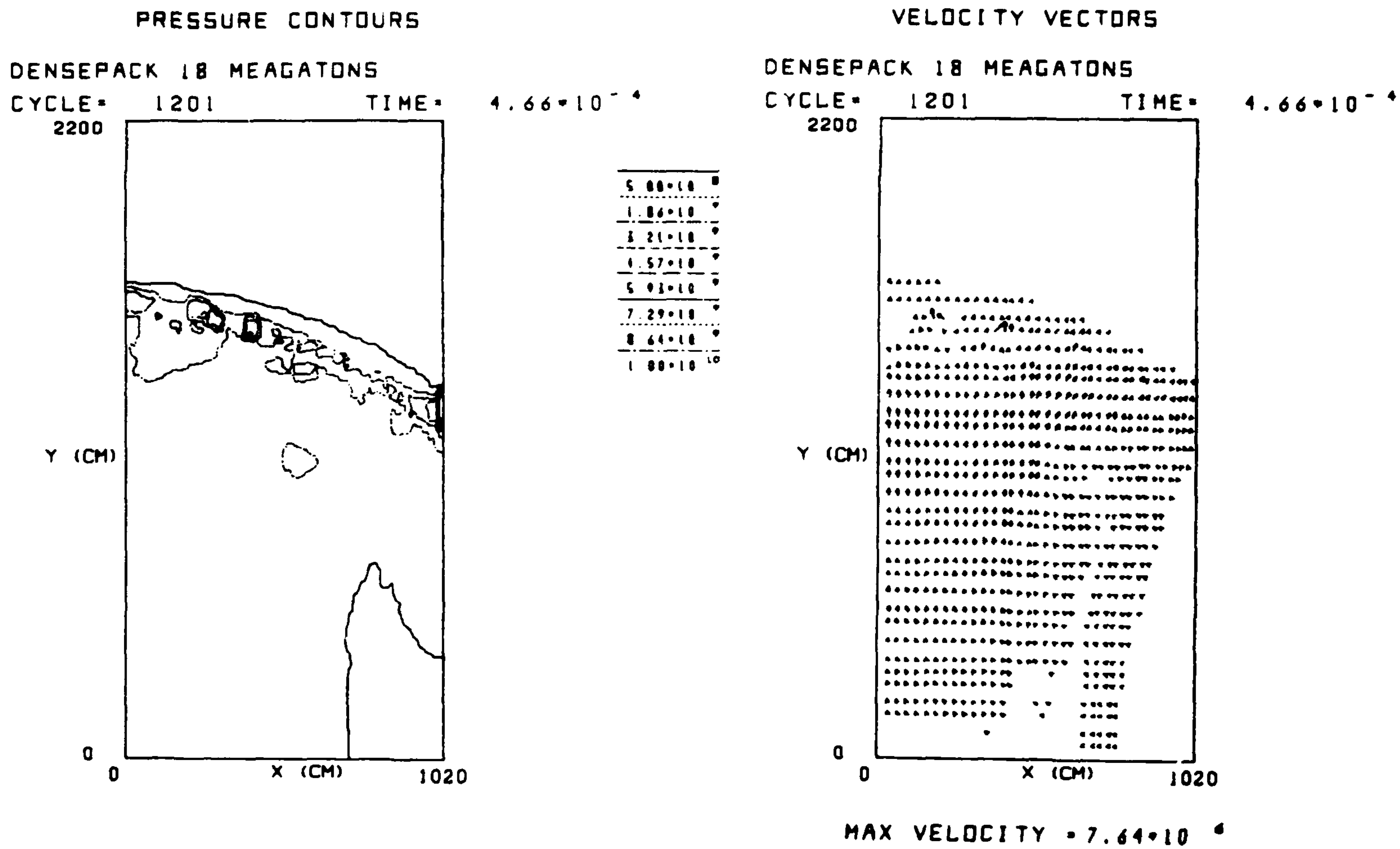

Fig. 3m — Pressure contours and velocity vectors calculated using FAST2D, shown at intervals of 100 cycles

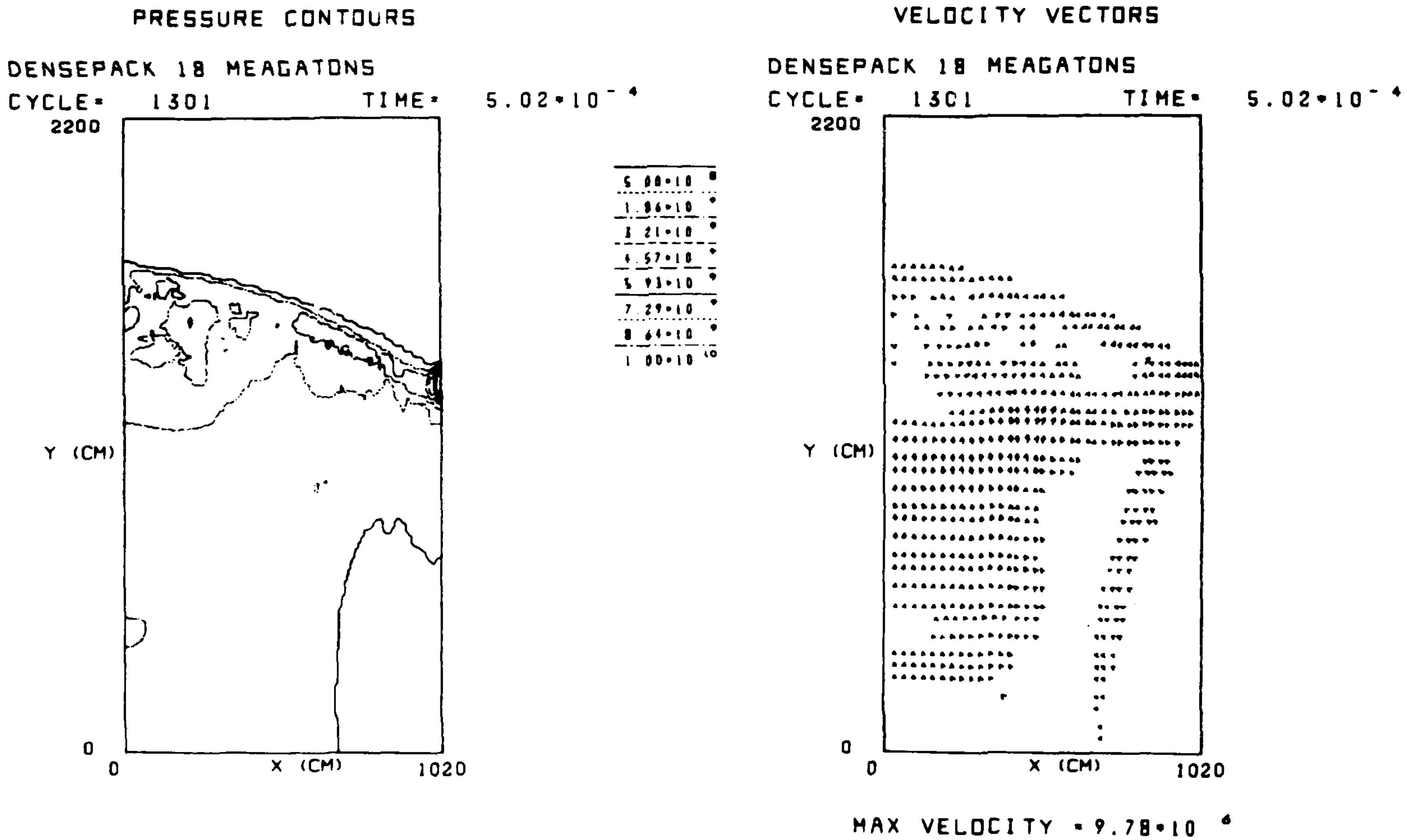

Fig. 3n — Pressure contours and velocity vectors calculated using FAST2D, shown at intervals of 100 cycles

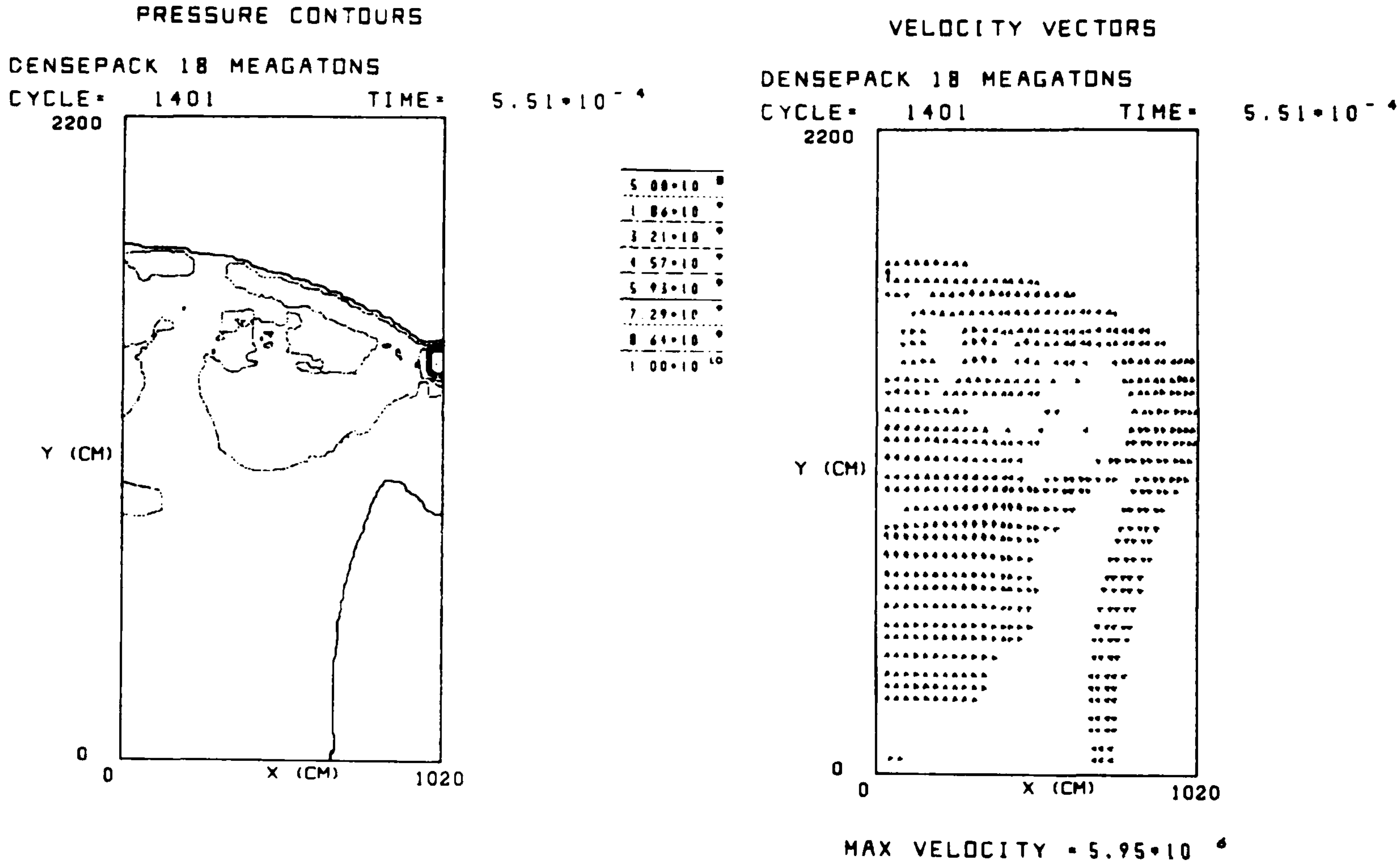

Fig. 3o — Pressure contours and velocity vectors calculated using FAST2D, shown at intervals of 100 cycles

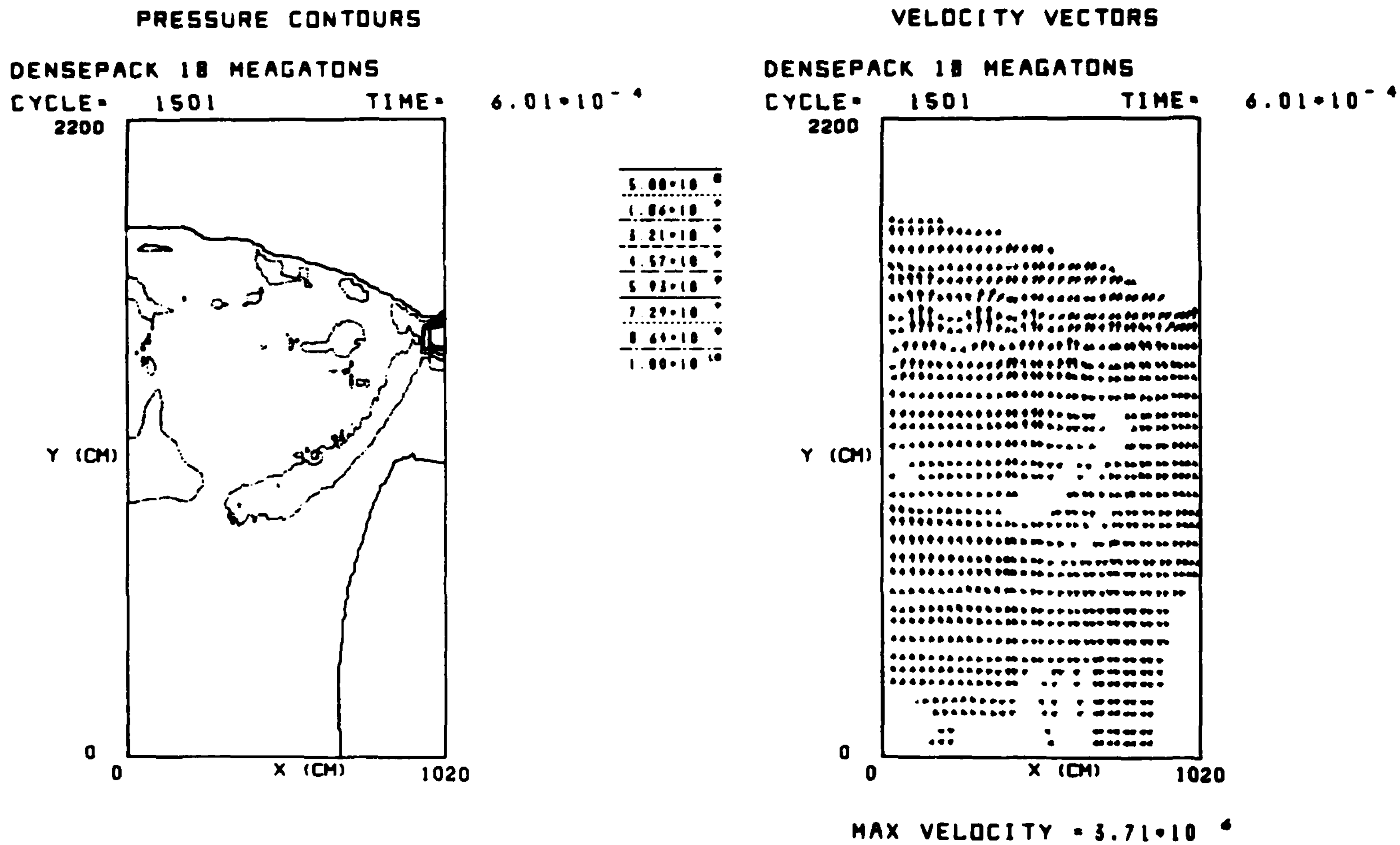

Fig. 3p — Pressure contours and velocity vectors calculated using FAST2D, shown at intervals of 100 cycles

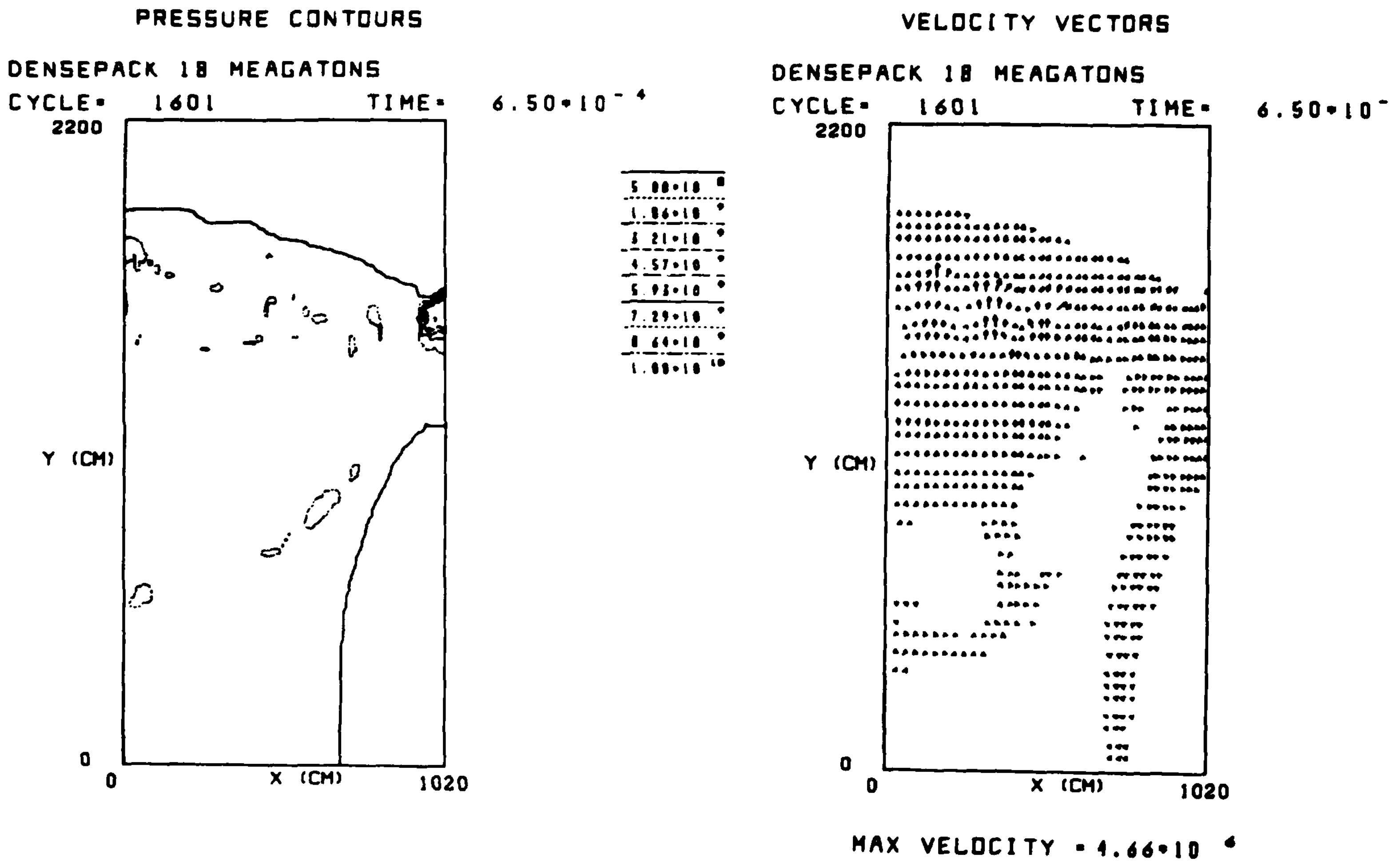

Fig. 3q — Pressure contours and velocity vectors calculated using FAST2D, shown at intervals of 100 cycles

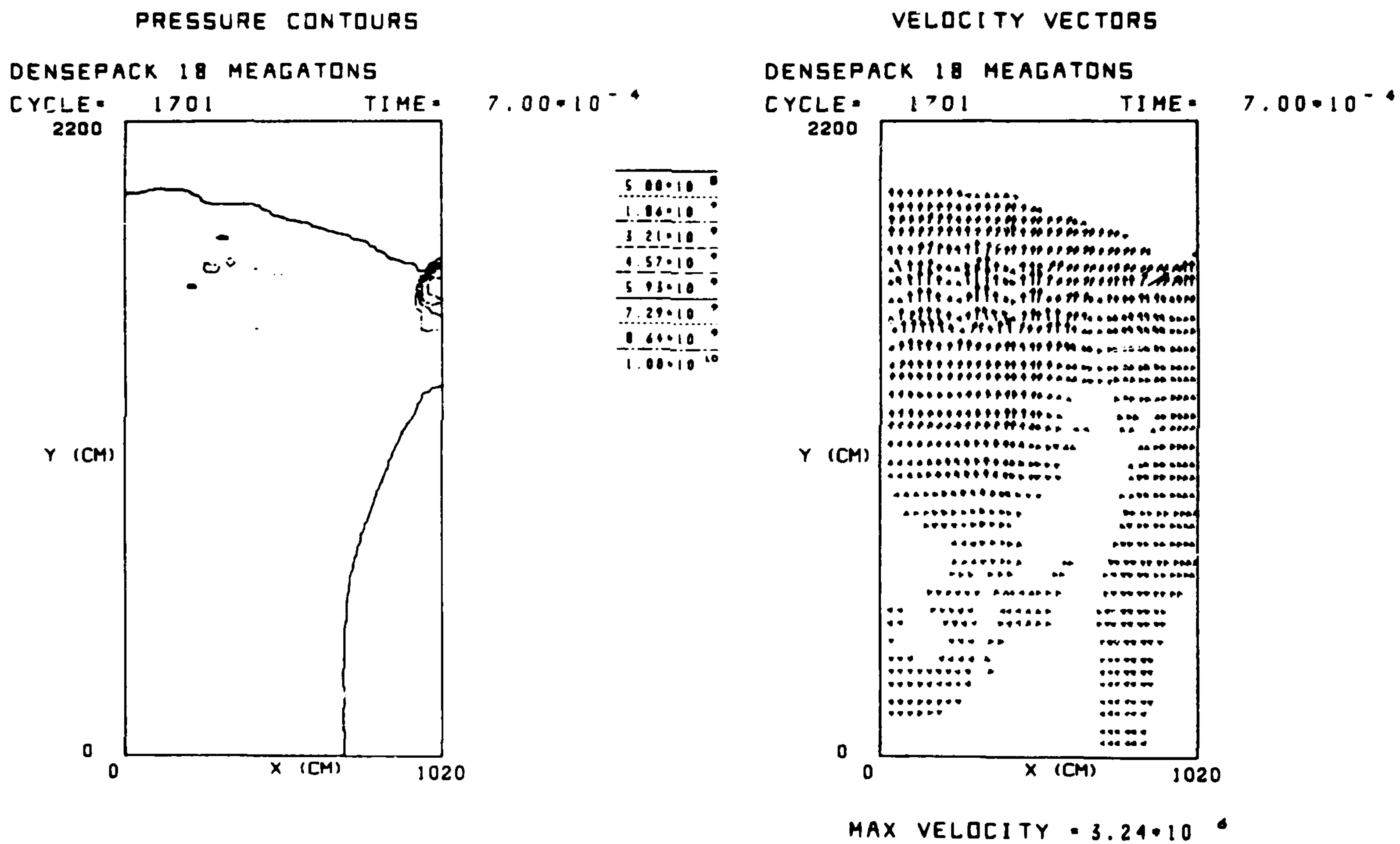

Fig. 3r — Pressure contours and velocity vectors calculated using FAST2D, shown at intervals of 100 cycles

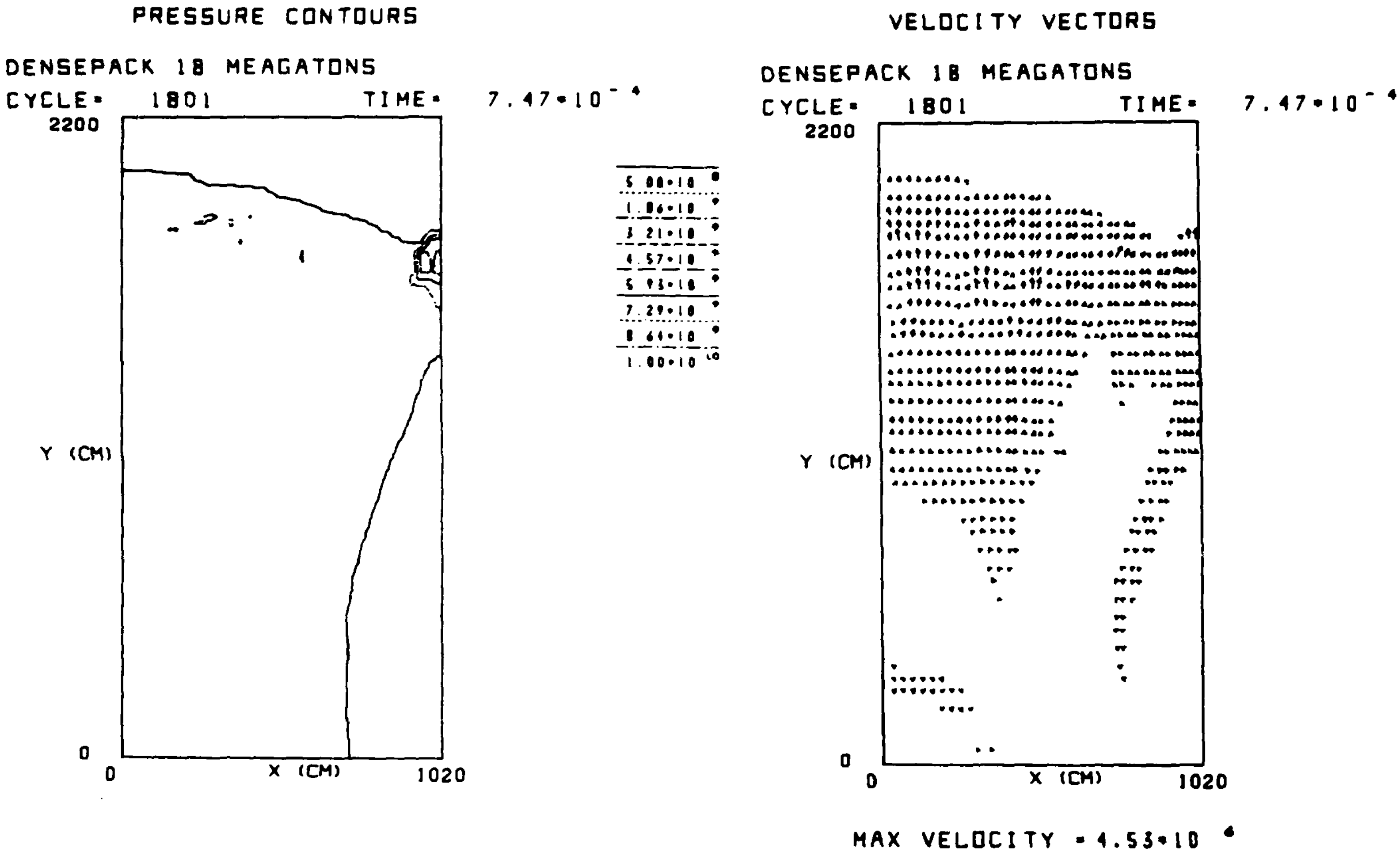

Fig. 3s — Pressure contours and velocity vectors calculated using FAST2D, shown at intervals of 100 cycles

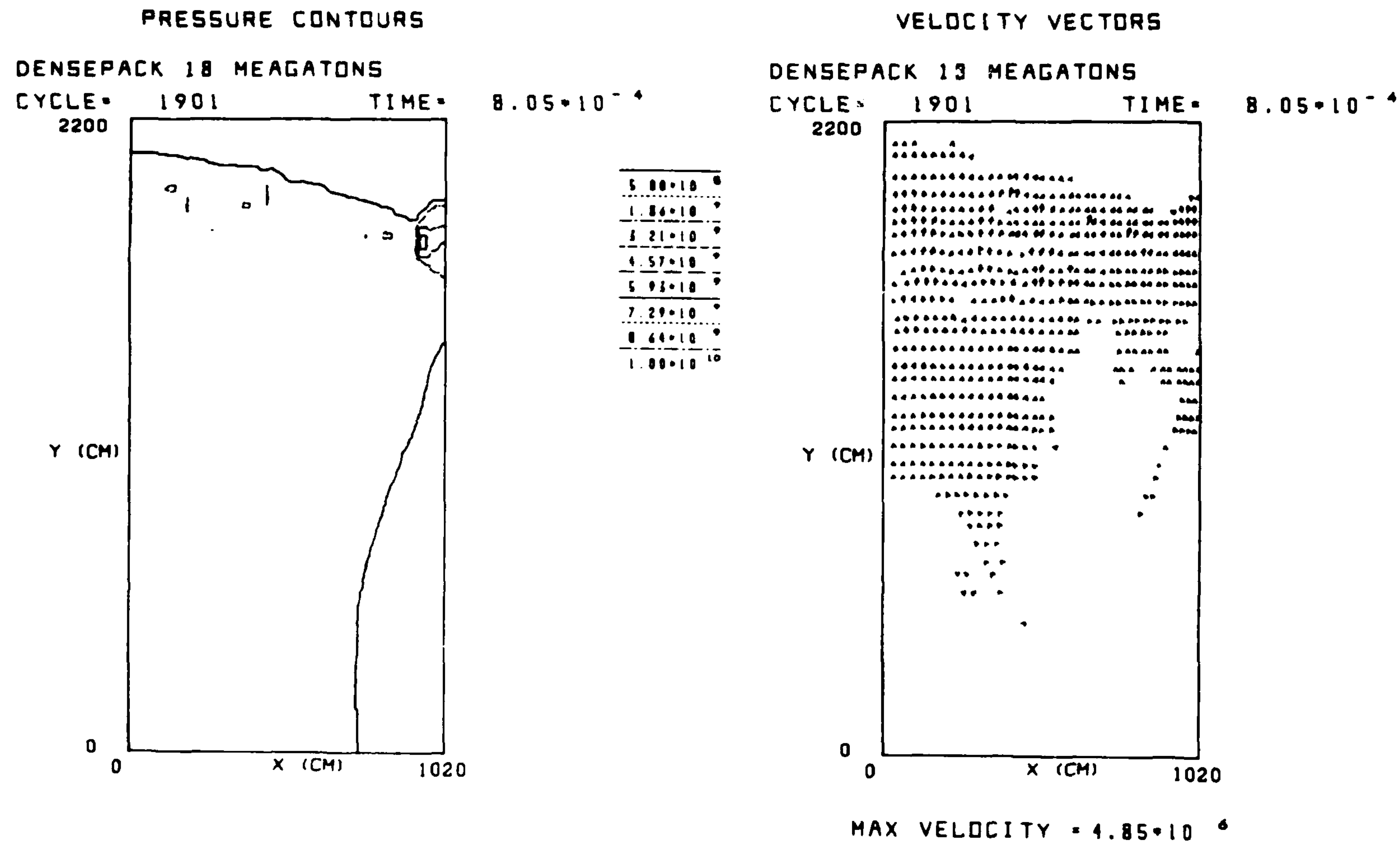

Fig. 3t — Pressure contours and velocity vectors calculated using FAST2D, shown at intervals of 100 cycles

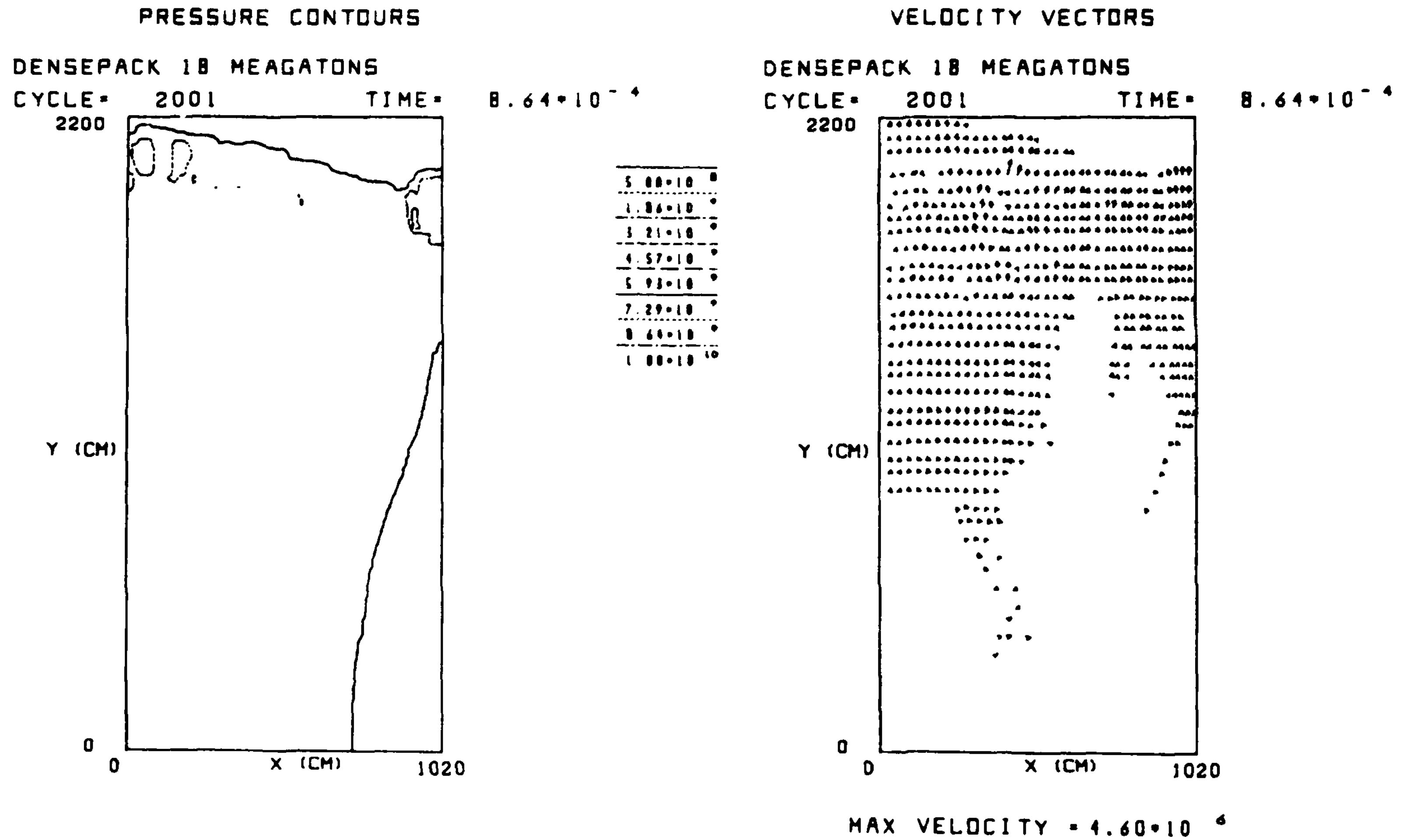

Fig. 3u — Pressure contours and velocity vectors calculated using FAST2D, shown at intervals of 100 cycles

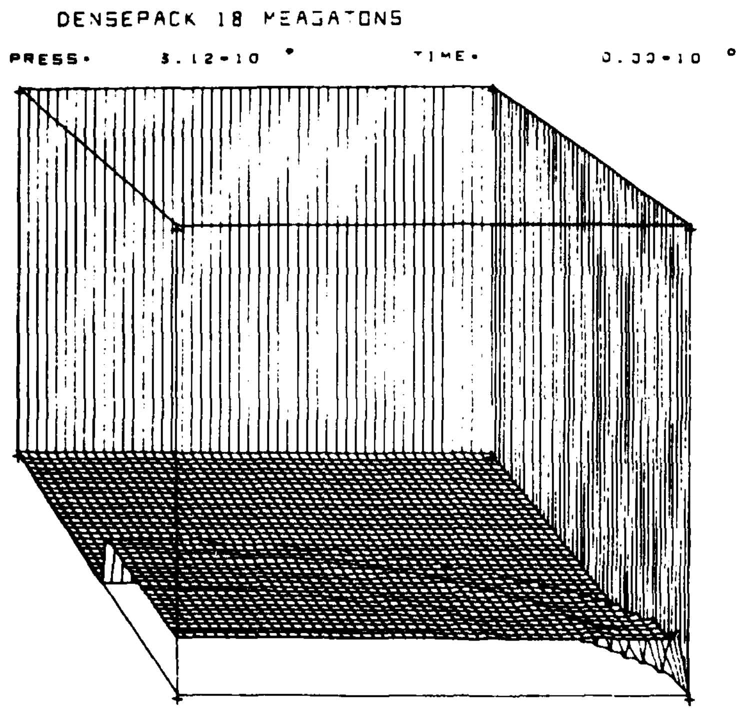

Fig. 4a — Pressure contours of Fig. 3, shown in orthographic projection. The pressure scale here is 22 kbar.

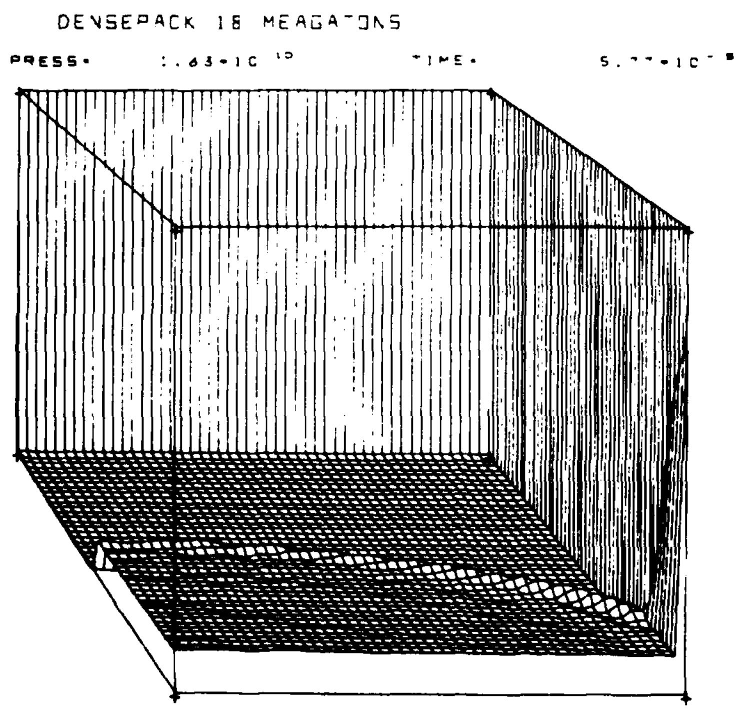

Fig. 4b — Pressure contours of Fig. 3, shown in orthographic projection. The pressure scale here is 22 kbar.

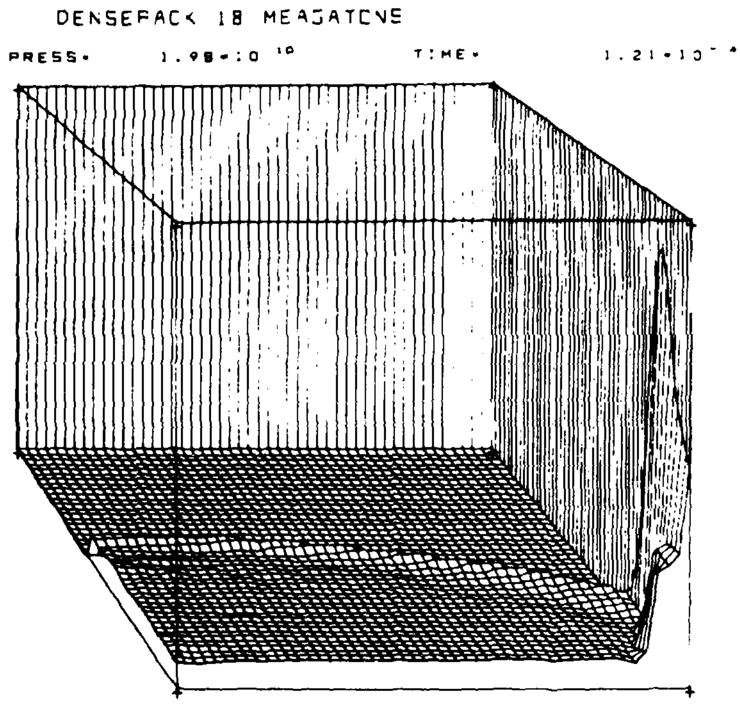

Fig. 4c — Pressure contours of Fig. 3, shown in orthographic projection. The pressure scale here is 22 kbar.

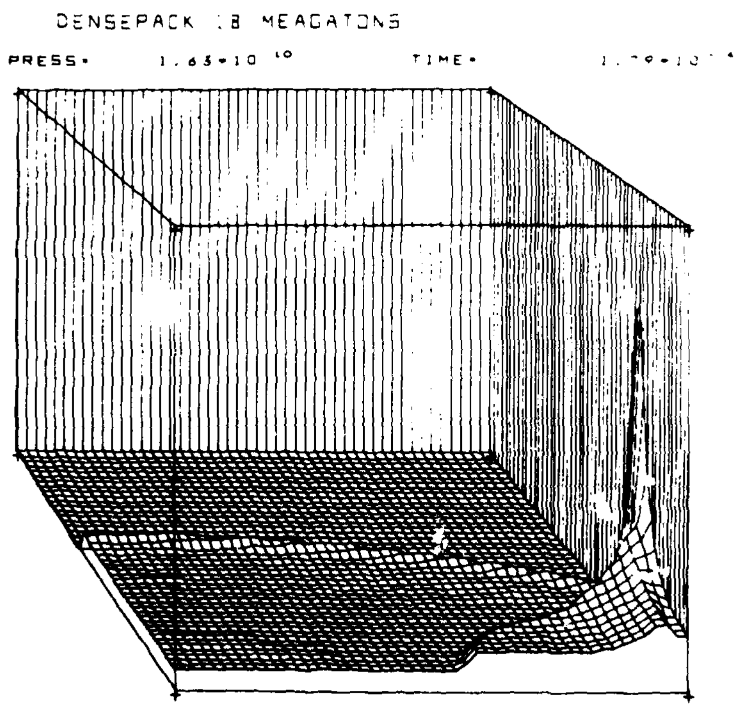

Fig. 4d — Pressure contours of Fig. 3, shown in orthographic projection. The pressure scale here is 22 kbar.

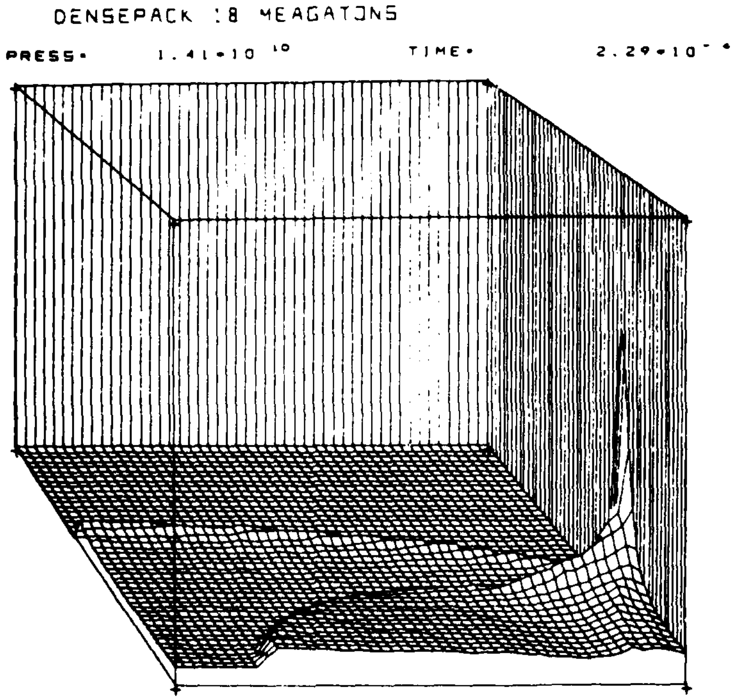

Fig. 4e — Pressure contours of Fig. 3, shown in orthographic projection. The pressure scale here is 22 kbar.

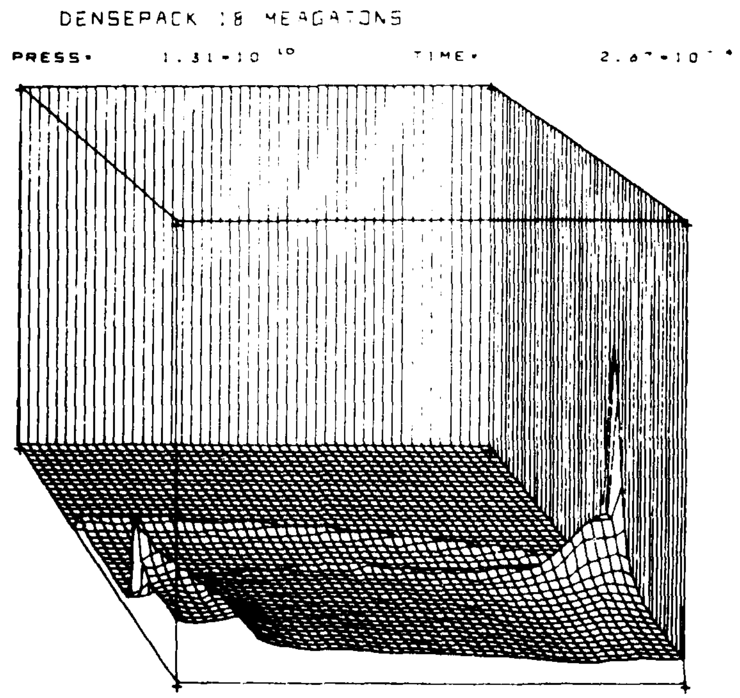

Fig. 4f — Pressure contours of Fig. 3, shown in orthographic projection. The pressure scale here is 22 kbar.

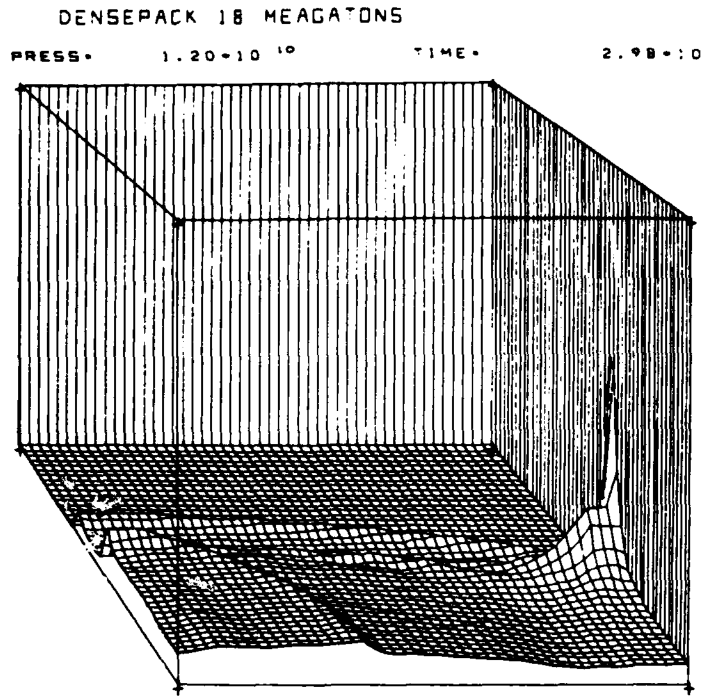

Fig. 4g — Pressure contours of Fig. 3, shown in orthographic projection. The pressure scale here is 22 kbar.

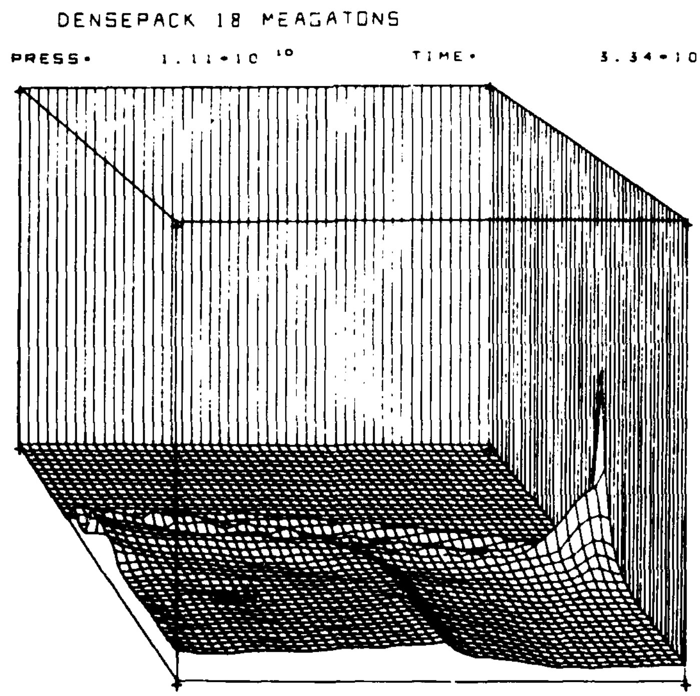

Fig. 4h — Pressure contours of Fig. 3, shown in orthographic projection. The pressure scale here is 22 kbar.

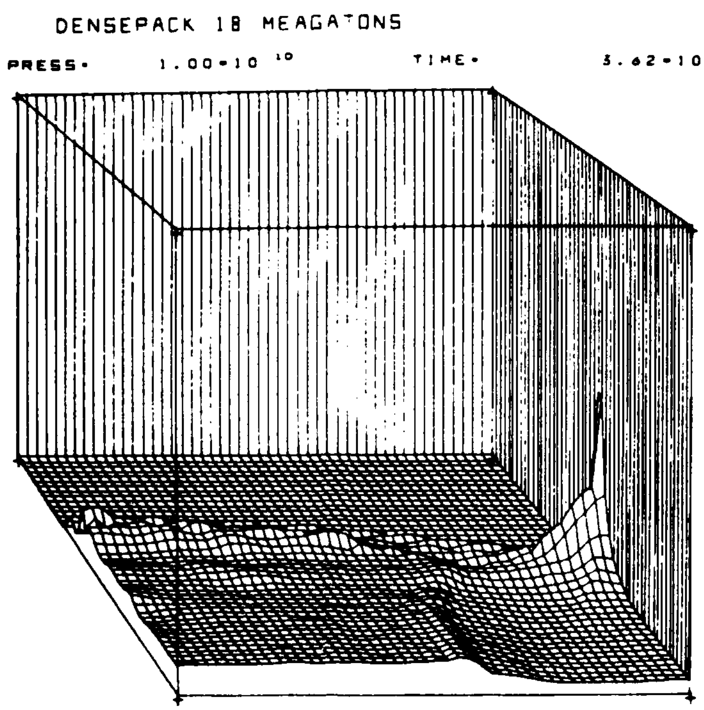

Fig. 4i — Pressure contours of Fig. 3, shown in orthographic projection. The pressure scale here is 22 kbar.

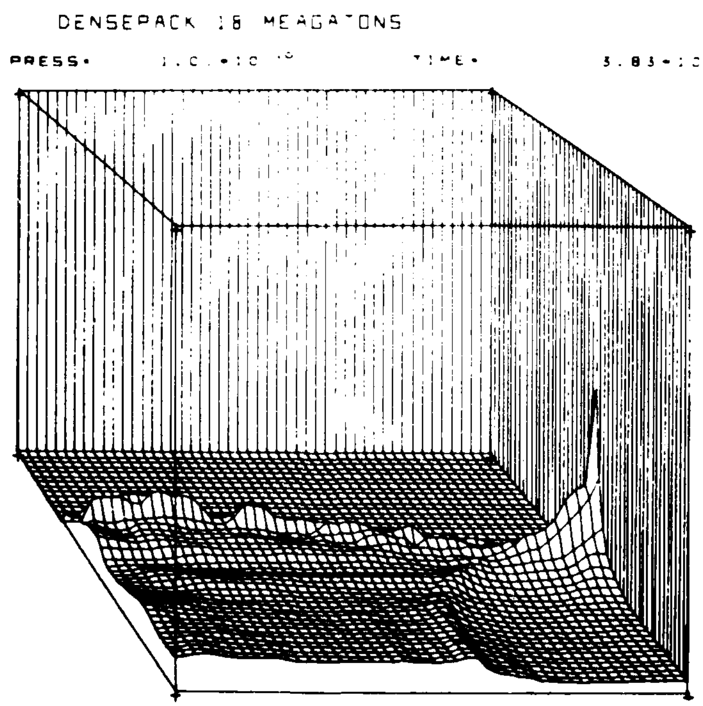

Fig. 4j — Pressure contours of Fig. 3, shown in orthographic projection. The pressure scale here is 22 kbar.

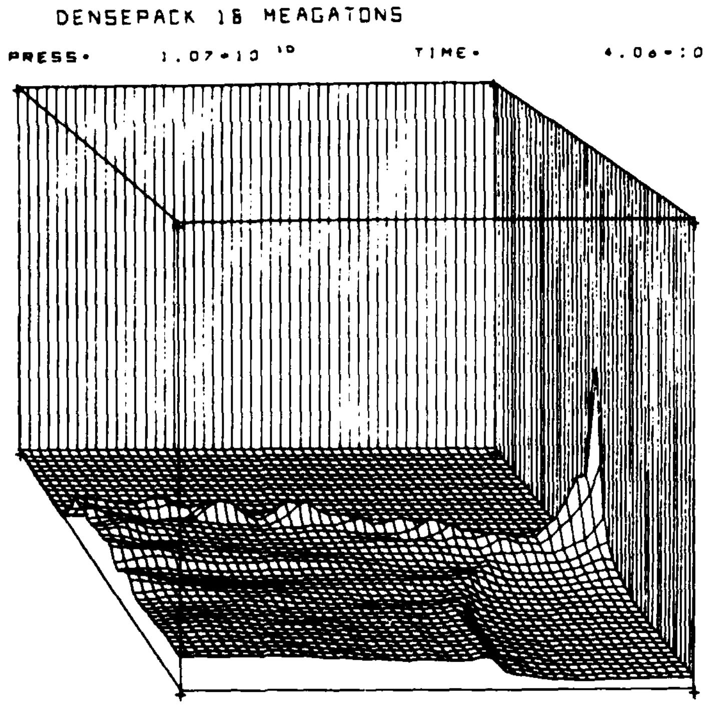

Fig. 4k — Pressure contours of Fig. 3, shown in orthographic projection. The pressure scale here is 22 kbar.

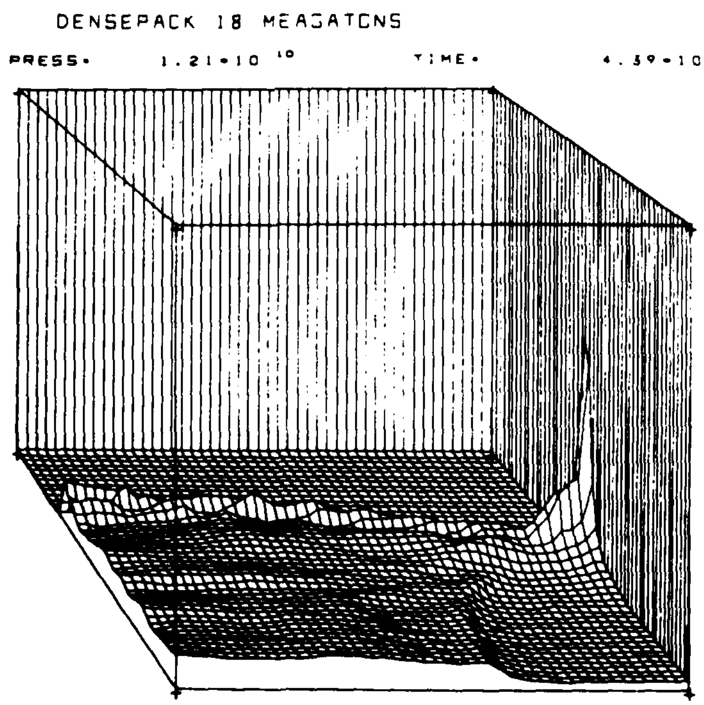

Fig. 4l — Pressure contours of Fig. 3, shown in orthographic projection. The pressure scale here is 22 kbar.

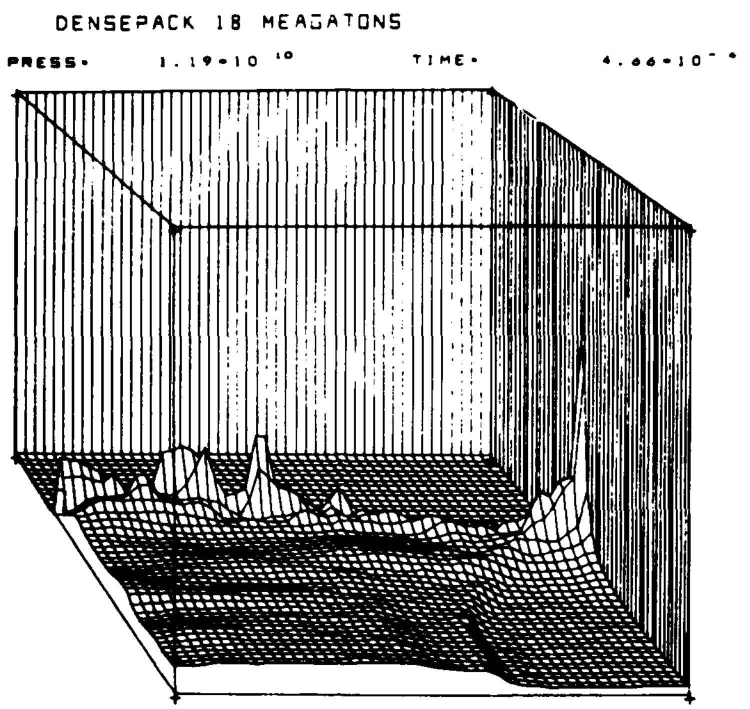

Fig. 4m — Pressure contours of Fig. 3, shown in orthographic projection. The pressure scale here is 22 kbar.

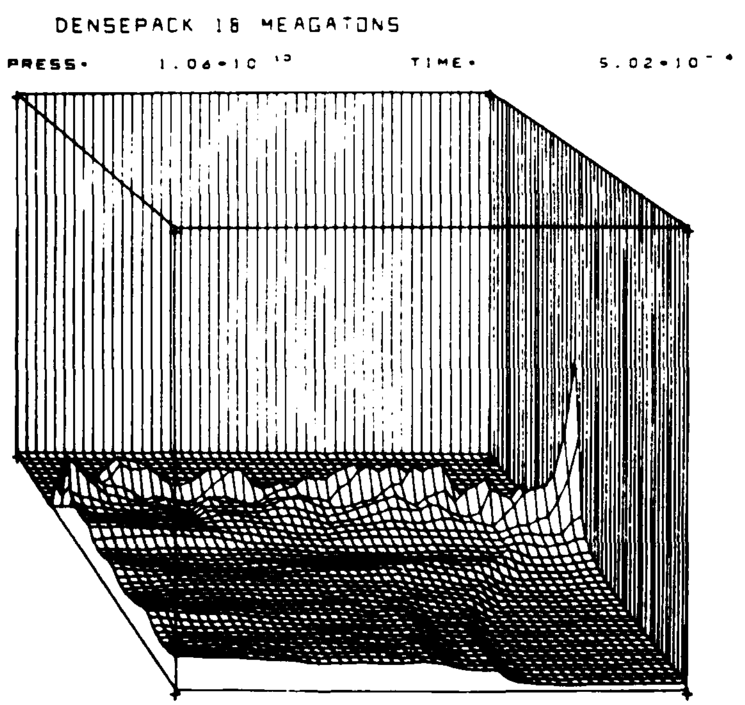

Fig. 4n — Pressure contours of Fig. 3, shown in orthographic projection. The pressure scale here is 22 kbar.

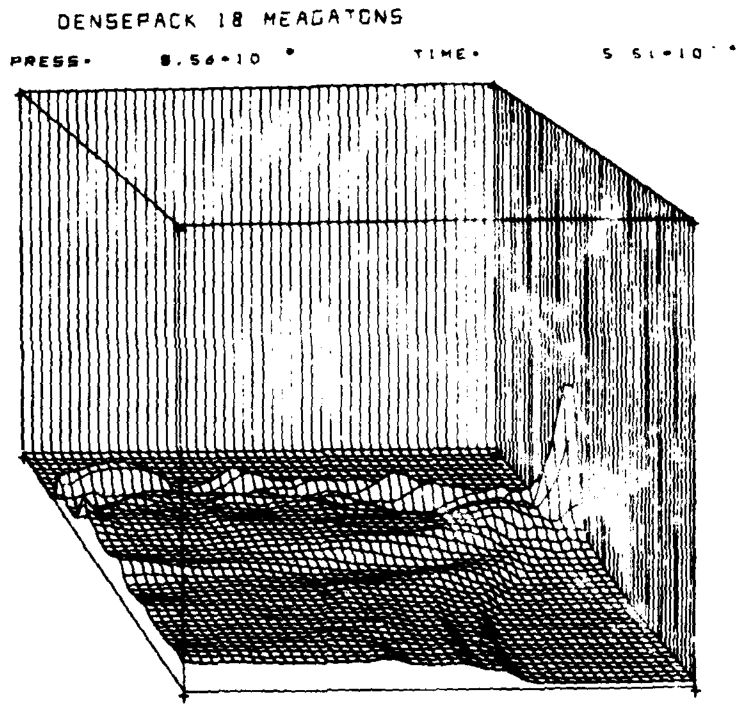

Fig. 4o — Pressure contours of Fig. 3, shown in orthographic projection. The pressure scale here is 22 kbar.

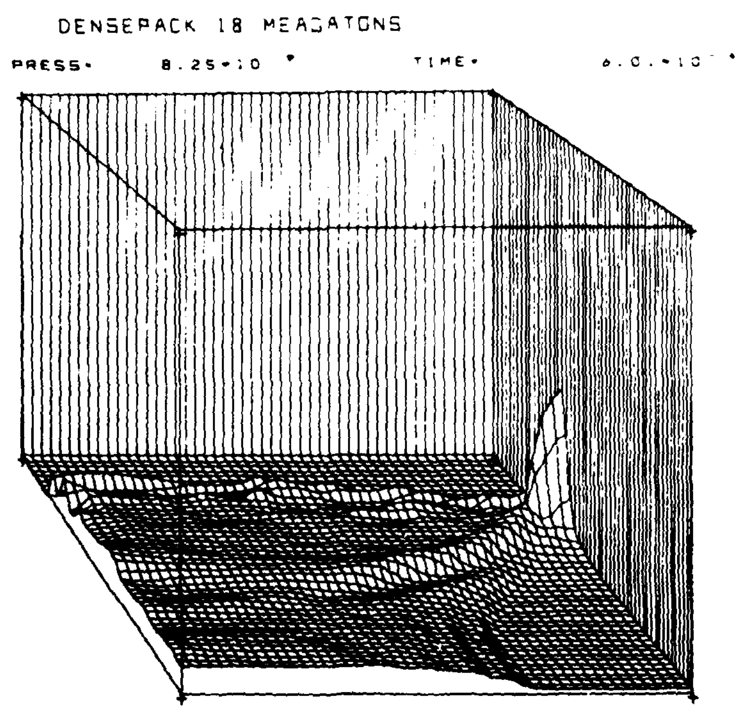

Fig. 4p — Pressure contours of Fig. 3, shown in orthographic projection. The pressure scale here is 22 kbar.

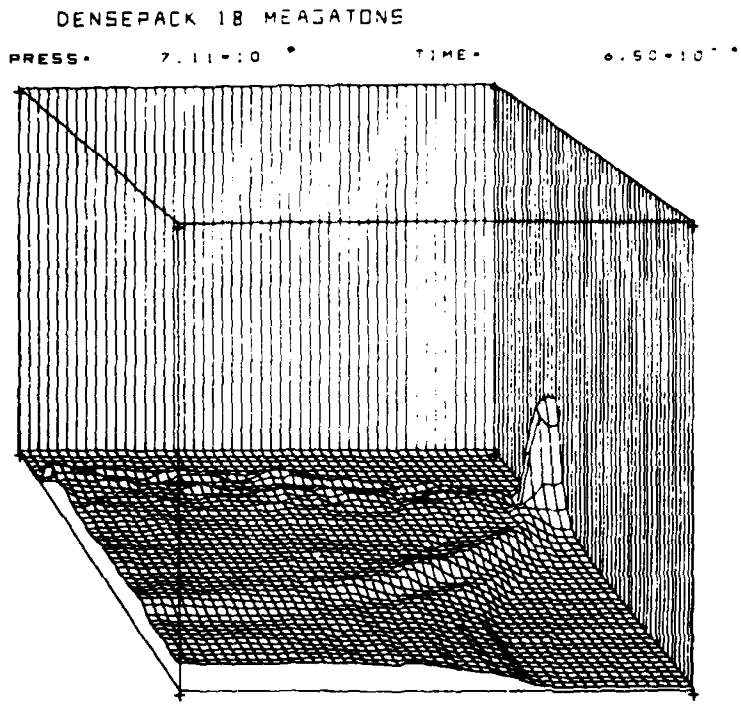

Fig. 4q — Pressure contours of Fig. 3, shown in orthographic projection. The pressure scale here is 22 kbar.

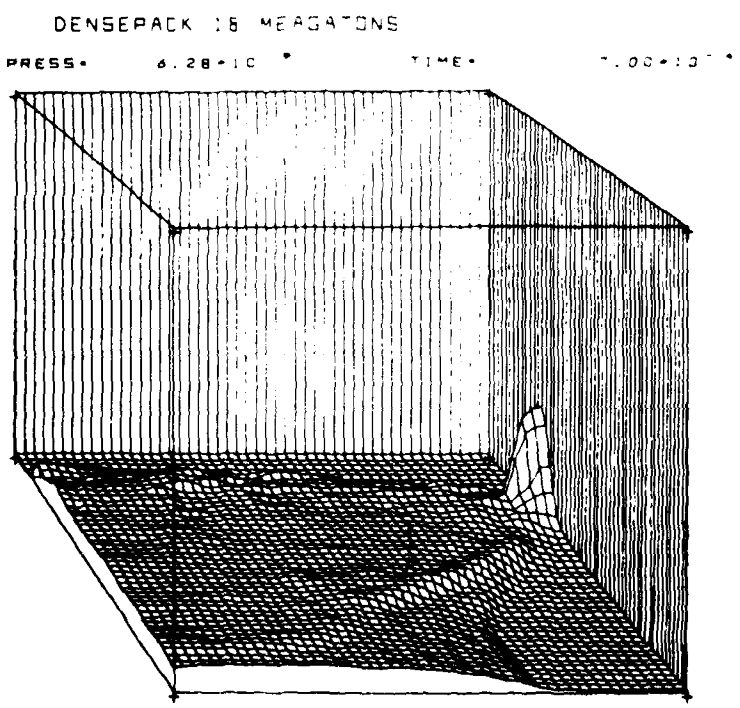

Fig. 4r — Pressure contours of Fig. 3, shown in orthographic projection. The pressure scale here is 22 kbar.

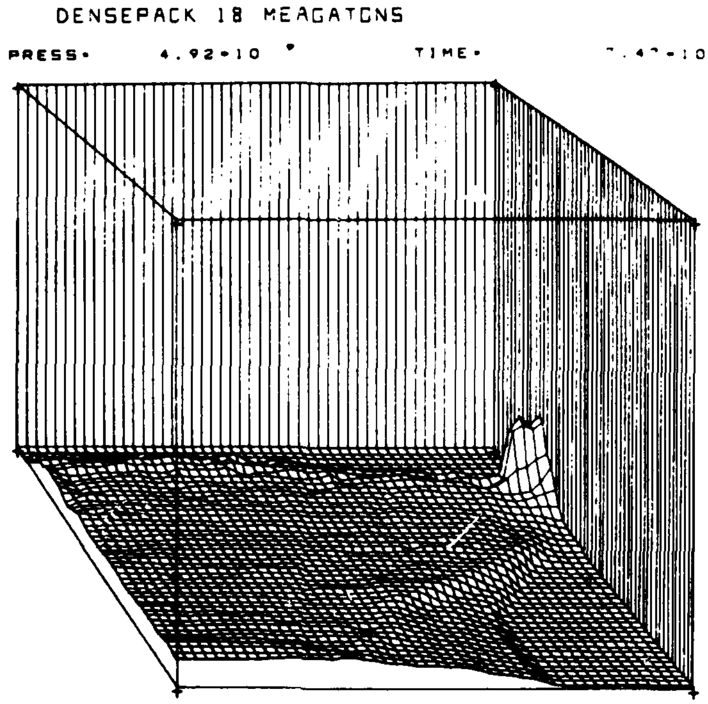

Fig. 4s — Pressure contours of Fig. 3, shown in orthographic projection. The pressure scale here is 22 kbar.

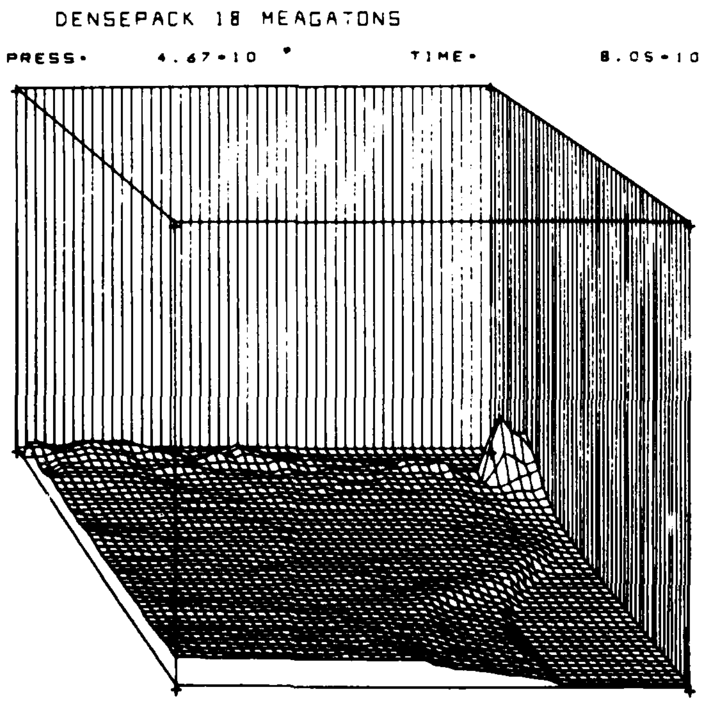

Fig. 4t — Pressure contours of Fig. 3, shown in orthographic projection. The pressure scale here is 22 kbar.

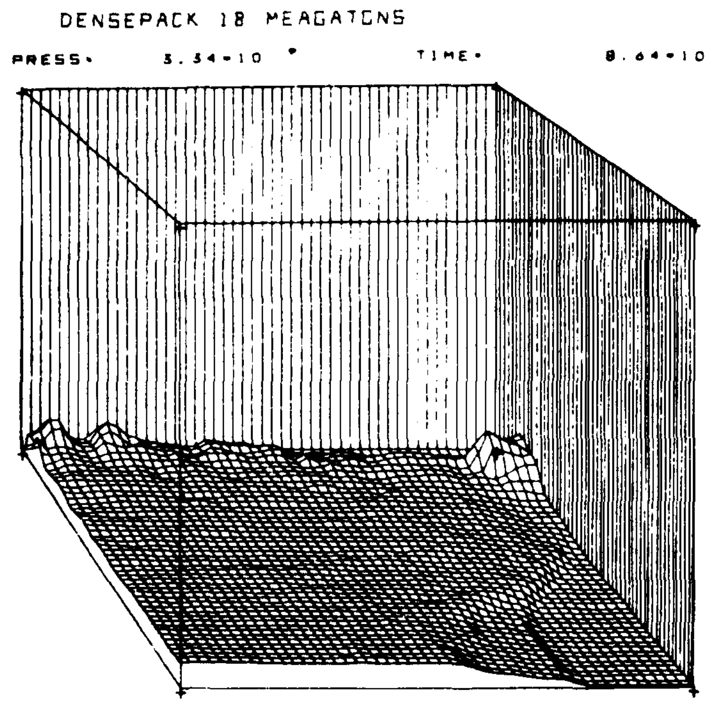

Fig. 4u — Pressure contours of Fig. 3, shown in orthographic projection. The pressure scale here is 22 kbar.

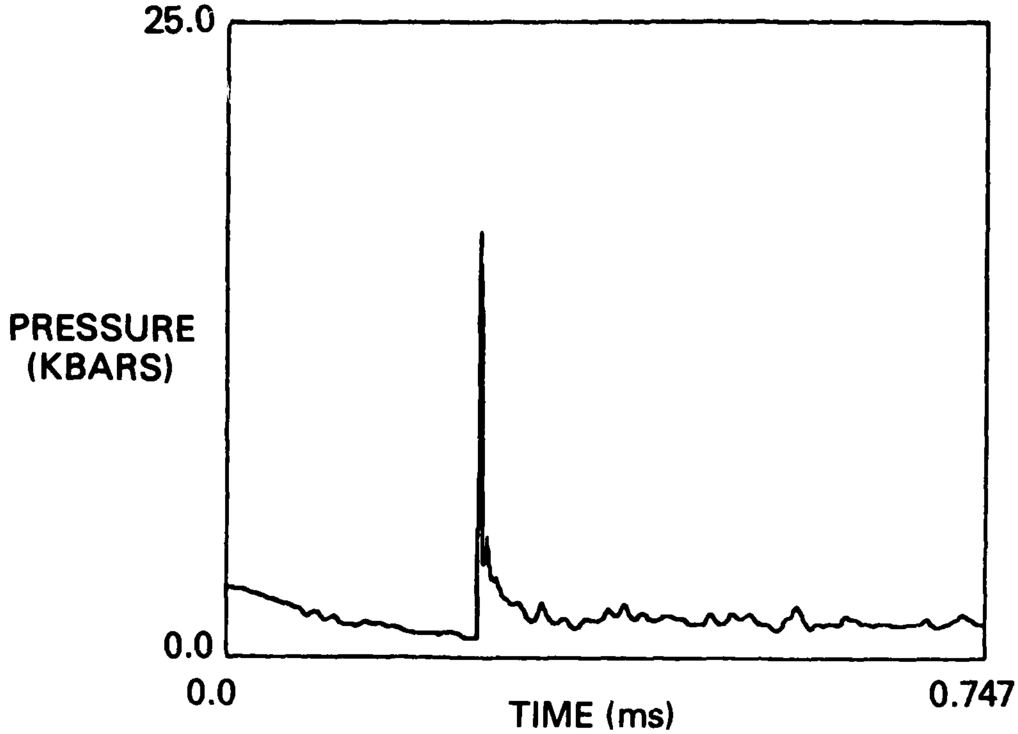

Fig. 5a — Pressure histories as measured by sensors located at radii of 0.0m

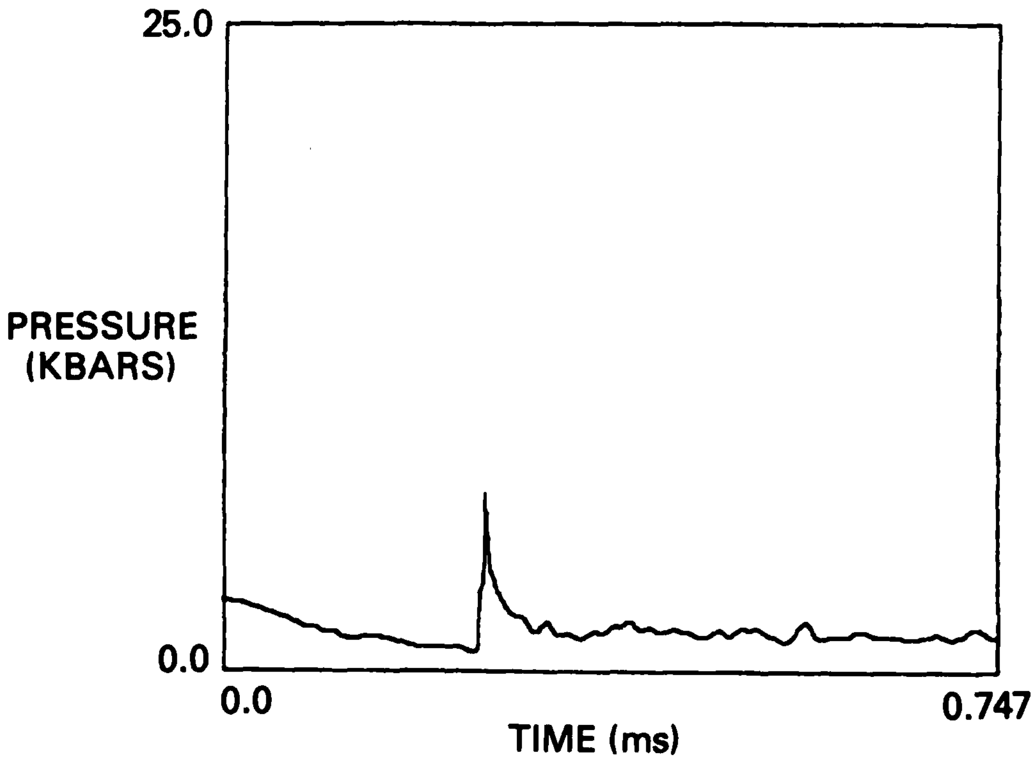

Fig. 5b — Pressure histories as measured by sensors located at radii of 0.035m

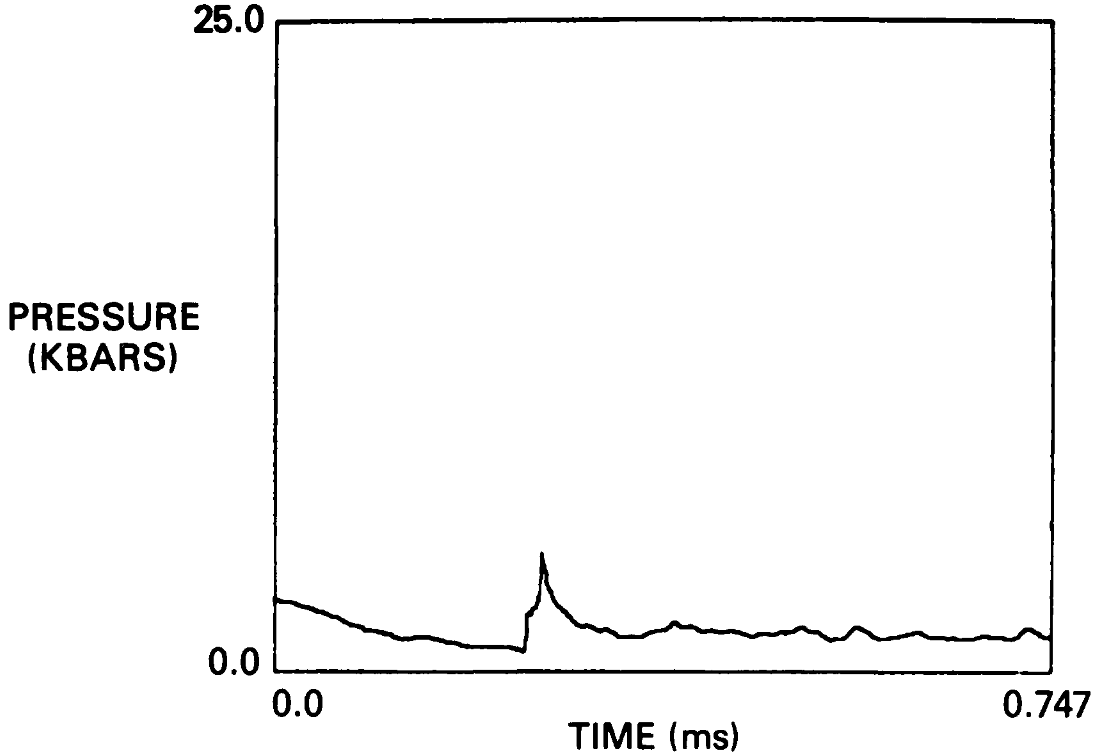

Fig. 5c — Pressure histories as measured by sensors located at radii of 0.075m

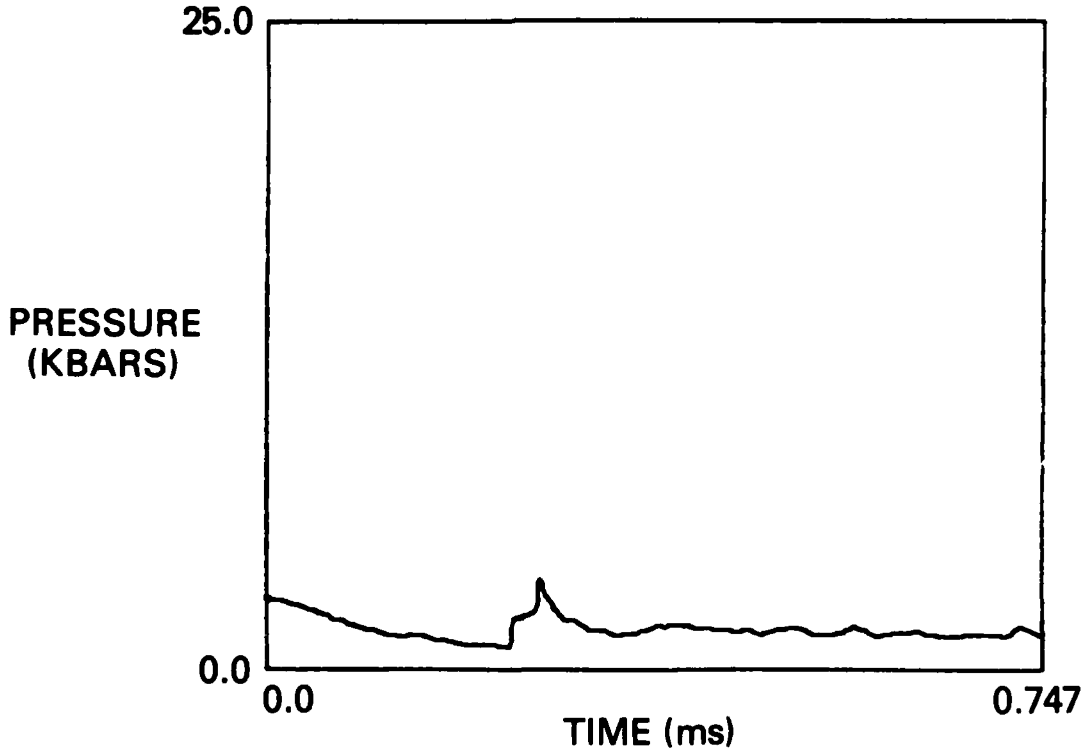

Fig. 5d — Pressure histories as measured by sensors located at radii of 1.25m

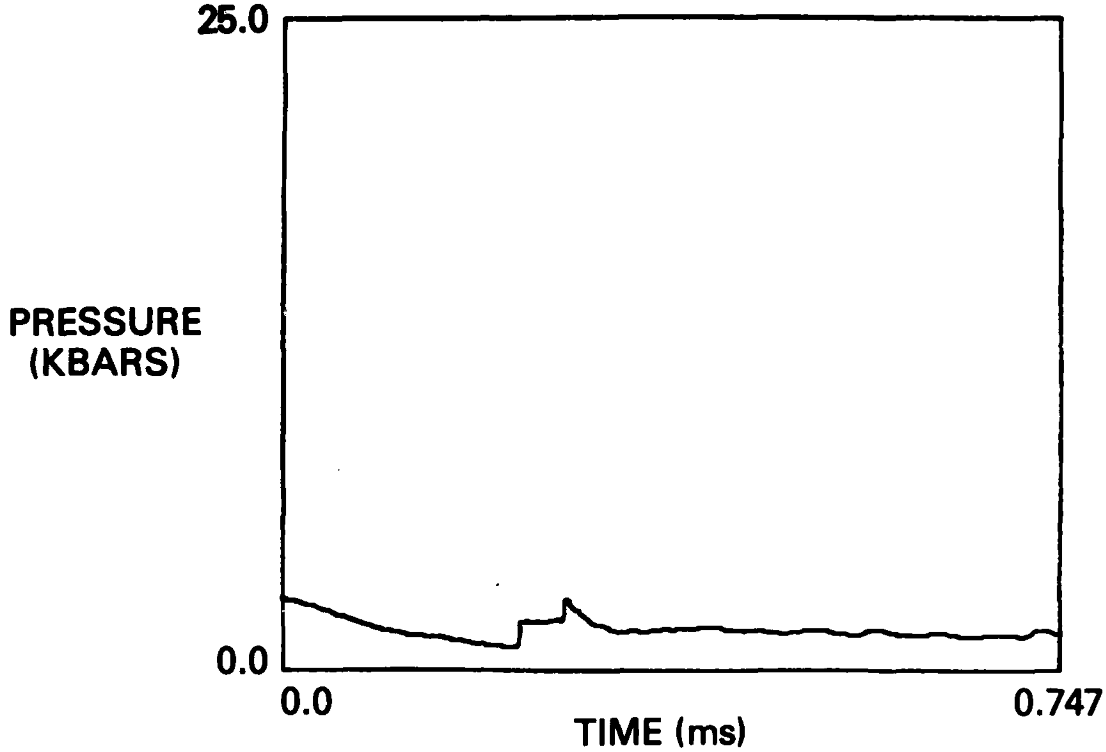

Fig. 5e — Pressure histories as measured by sensors located at radii of 2.0m

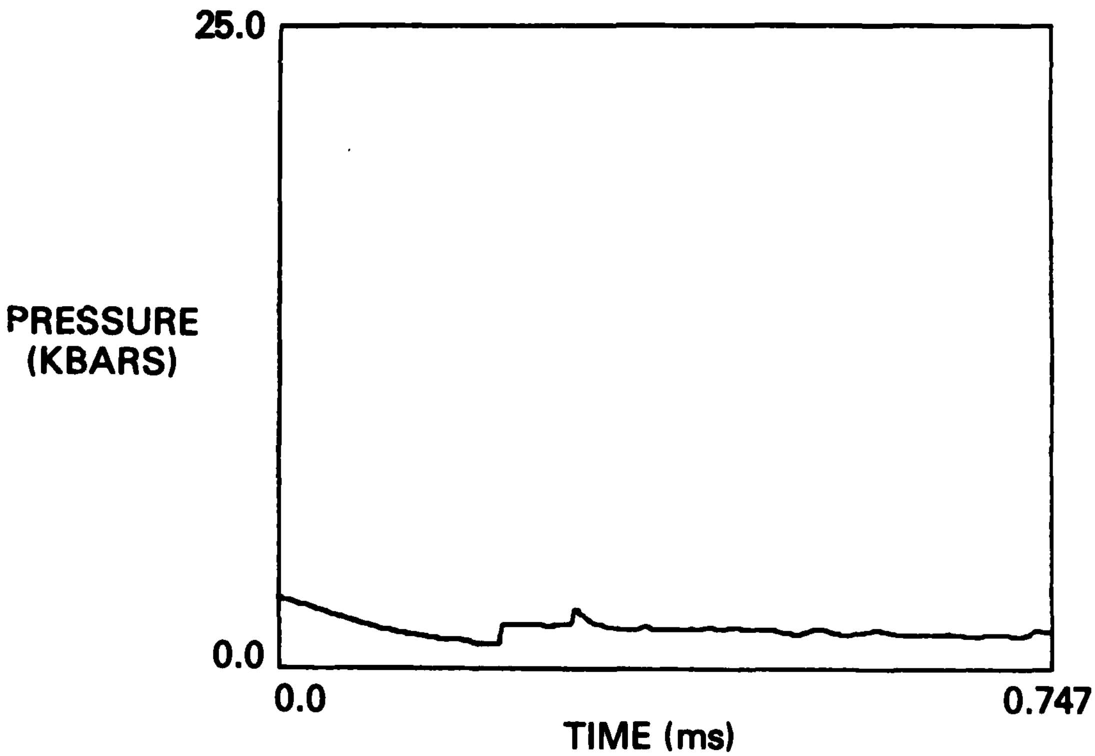

Fig. 5f — Pressure histories as measured by sensors located at radii of 3.0m

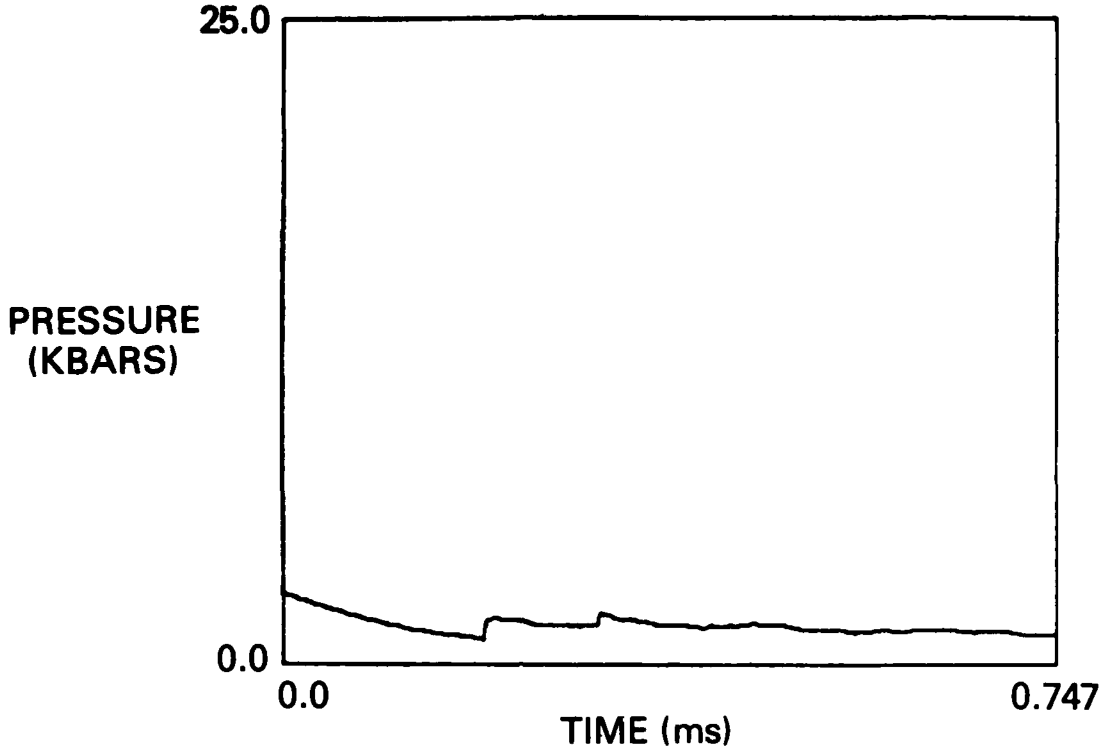

Fig. 5g — Pressure histories as measured by sensors located at radii of 4.5m

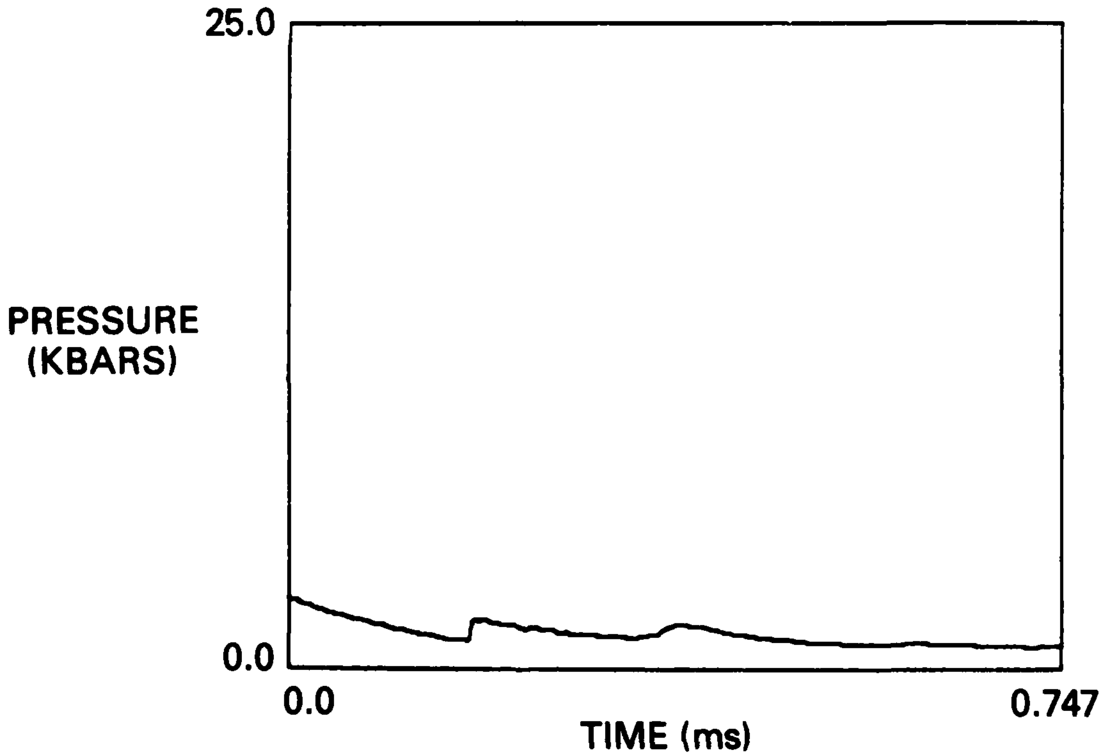

Fig. 5h — Pressure histories as measured by sensors located at radii of 6.05m

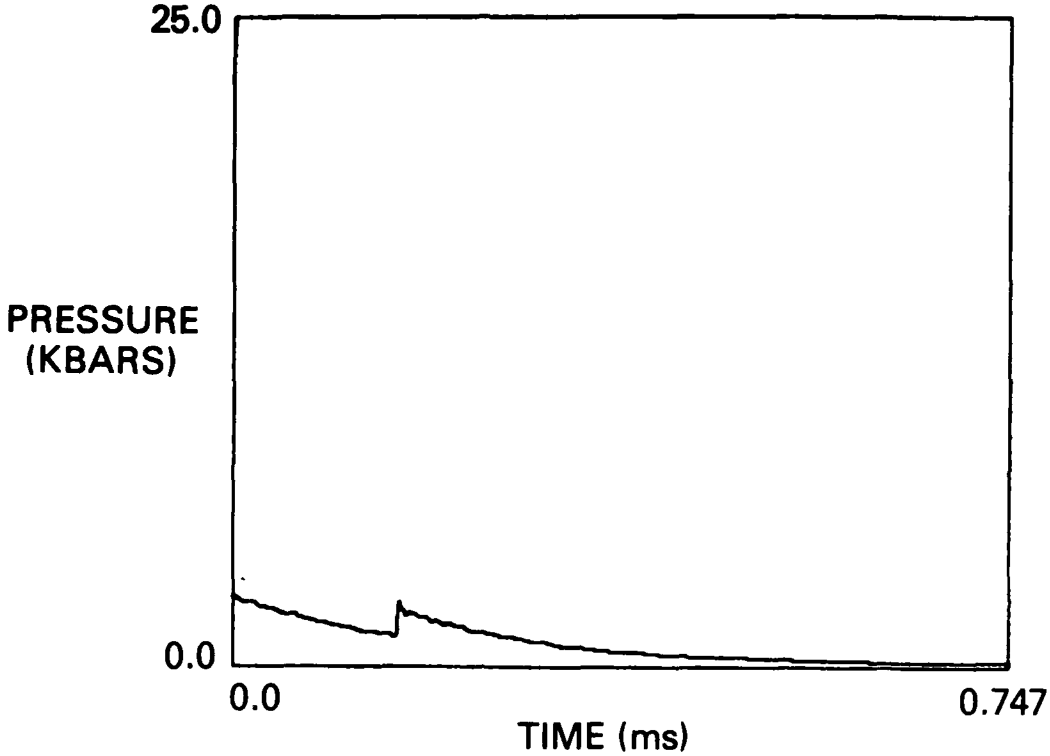

Fig. 5i — Pressure histories as measured by sensors located at radii of 7.5m

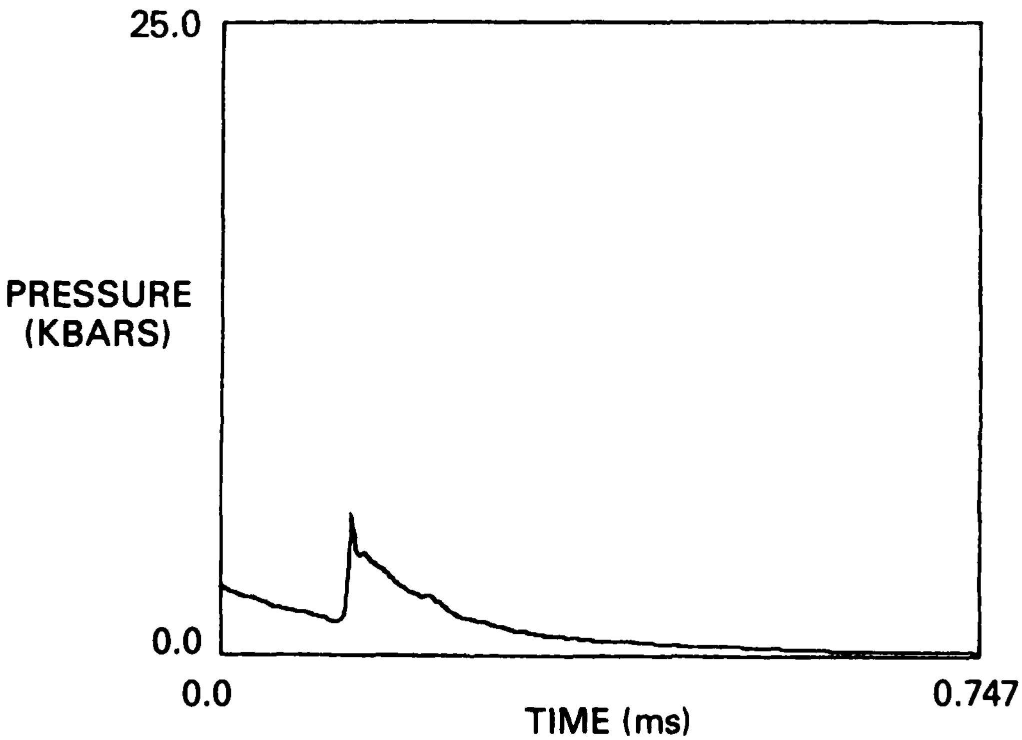

Fig. 5j — Pressure histories as measured by sensors located at radii of 9.25m

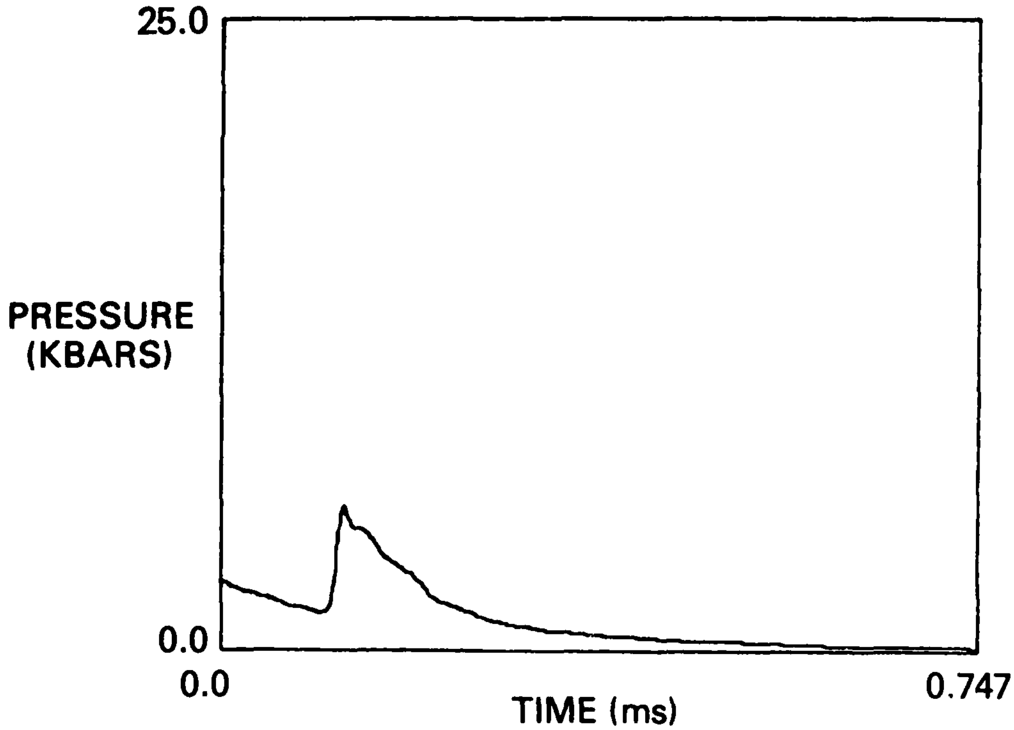

Fig. 5k — Pressure histories as measured by sensors located at radii of 9.5m

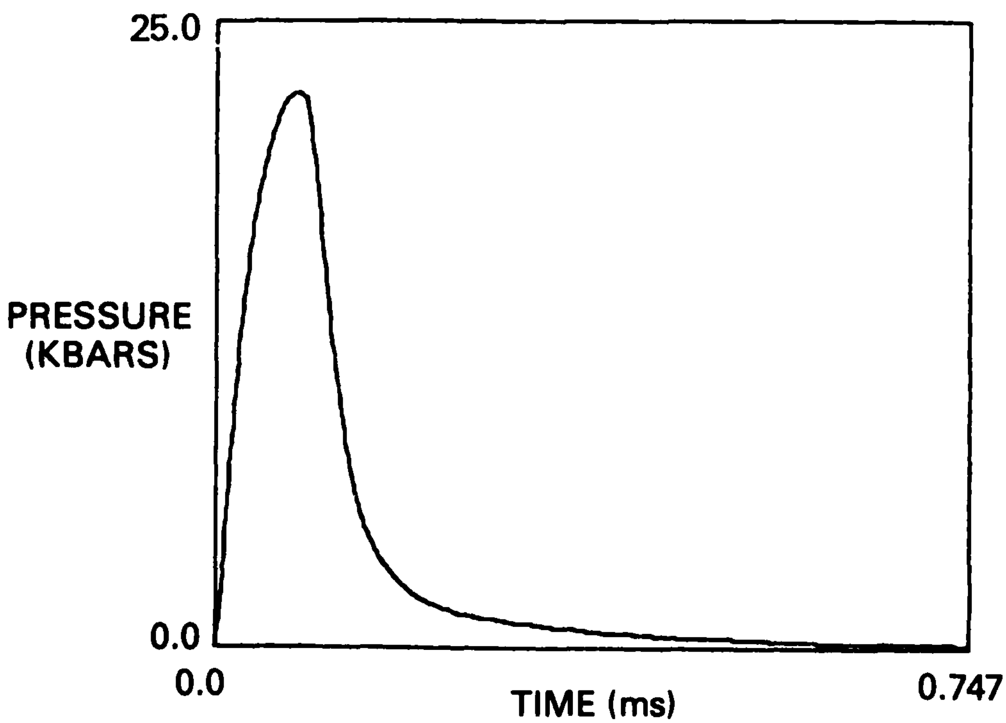

Fig. 5l — Pressure histories as measured by sensors located at radii of 10.0m

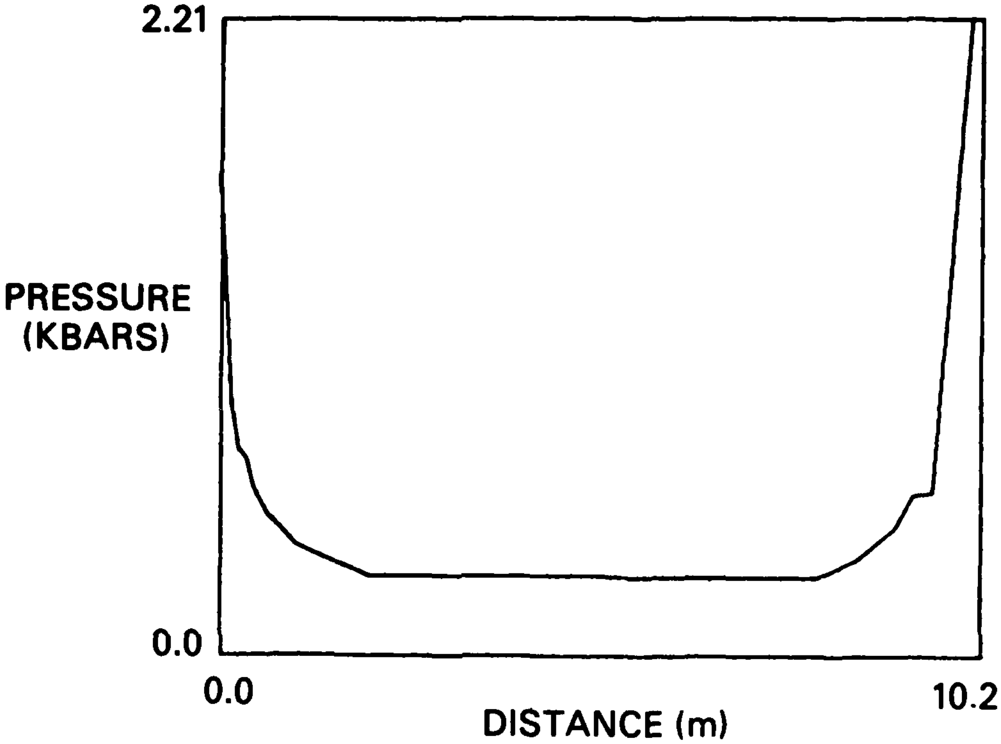

Fig. 6 — Maximum recorded station pressure in kbar as function of station radial location

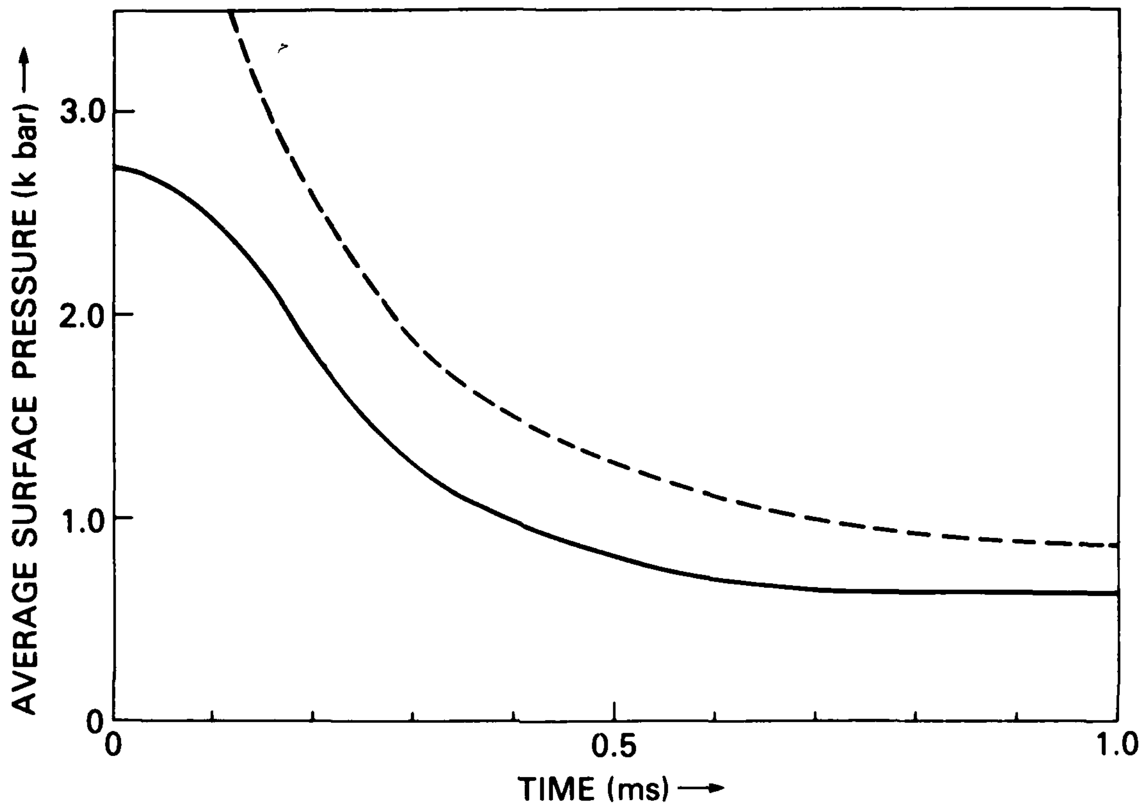

Fig. 7 — Average pressure on floor of mesh (solid curve) and pressure at origin calculated from Sedov one-dimensional self-similar solution with $\gamma = 1.2$ (broken curve) as functions of time

REFERENCES

1. Latter, Albert (1982, unpublished).

2. Sedov, L. I., Similarity and Dimensional Methods in Mechanics, Academic Press, New York (1959), p. 220.

3. Fry, M. A., Picone, J. M., Boris, J. P., and Book, D. B., "Transition to Double Mach Stem for Nuclear Explosion at 104FT Height of Burst", NRL Memorandum Report #4630 (1981).

4. Carpenter, H. J., "Height-of-Burst Blast at High Overpressure," 4th International Symposium on Military Applications of Blast Simulation (1974).

5. Pyatt, K., CSB Review Meeting, DNA Hadquarters, October 13, 1982.

DISTRIBUTION LIST

Assistant to the Secretary of Defense
Atomic Energy
Washington, DC 20301
Olcy Attn Executive Assistant

Director
Defense Advanced Rsch Proj Agency
1400 Wilson Blvd
Arlington, VA 22209
(desires only one copy to library)
Olcy Attn TIO

Director
Defense Communications Agency
Washington, DC 20305
(ADR CNWDI: Attn Code 240 for)
Olcy Attn Code 670 R LIPP

Director
Defense Intelligence Agency
Washington, DC 20301
Olcy Attn DB-4C E OFARREL
Olcy Attn DB-4N
Olcy Attn DT-1C
Olcy Attn DT-2
Olcy Attn RDS-3A (TECH LIB)

Director
Defense Nuclear Agency
Washington, DC 20305
02cy Attn SPSS
04cy Attn TITL
Olcy Attn DDST

Defense Technical Information Center
Cameron Station
Alexandria, VA 22314
2cy Attn DD

Chairman
Department of Defense Explo Safety Board
Rm 856-C
Hoffman Building 1
2461 Eisenhower Avenue
Alexandria, VA 22331
Olcy Attn Chairman

Commander
Field Command
Defense Nuclear Agency
Kirtland AFB, NM 87115
Olcy Attn FCTMOF
Olcy Attn FCT
Olcy Attn FCPR

Chief
Field Command
Defense Nuclear Agency
Livermore Division
P O Box 808 L-317
Livermore, CA 94550
Olcy Attn FCPRL

Director
Joint Strat TGT Planning Staff
Offutt AFB
Omaha, NB 68113
Olcy Attn DOXT
Olcy Attn JLA
Olcy Attn JLTW-2
Olcy Attn NRI-STINFO Library
Olcy Attn XPFS

Commandant
Nato School (Shape)
APO New York, NY 09172
Olcy Attn U.S. Documents Officer

Under Secy of Def for Rsch & Engrg
Department of Defense
Washington, DC 20301
Olcy Attn Strategic & Space Systems (OS)

Director
BMD Advanced Technology Center
Department of the Army
P O Box 1500
Huntsville, AL 35807
Olcy Attn 1CRDABH-X
Olcy Attn ATC-T

Commander
BMD Systems Command
Department of the Army
P O Box 1500
Huntsville, AL 35807
Olcy Attn BMDSC-H N HURST

Chief of Engineers
Department of the Army
Forrestal Building
Washington, DC 20314
Olcy Attn DAEN-RDM
Olcy Attn DAEN-MCE-D

Deputy of Chief of Staff for
OPS & Plans
Department of the Army
Washington, DC 20310
Olcy Attn DAMO-NC

Commander
Harry Diamond Laboratories
Department of the Army
2800 Powder Mill Road
Adelphi, MD 20783
(CNWDI-Inner Envelope:
Attn: DELHD-RBH)
Olcy Attn Chief Div 20000
Olcy Attn DELHD-I-TL (Tech Lib)

Commander
U.S. Army Armament Material Readiness
Command
Rock Island, IL 61202
Olcy Attn MA Library

Director
U.S. Army Ballistic Research Labs
Aberdeen Proving Ground, MD 21005
Olcy Attn DRDAR-BLE J Keefer
02cy Attn DRDAR-TSB-S (Tech Lib)
Olcy Attn DRDAR-BLT W Taylor
Olcy Attn DRDAR-BLV

Commander
U.S. Army Communications Command
Fort Huachuca, AZ 85613
Olcy Attn Technical Reference Div

Commander
U.S. Army Concepts Analysis Agency
8120 Woodmont Avenue
Bethesda, MD 20014
Olcy Attn MOCA-ADL (Tech Lib)

Commander
U.S. Army Engineer Center
Fort Belvoir, VA 22060
Olcy Attn ATZA

Division Engineer
U.S. Army Engineer Div Huntsville
P O Box 1600, West Station
Huntsville, AL 35807
Olcy Attn HNDED-SR

Division Engineer
U.S. Army Engineer Div Ohio River
P O Box 1159
Cincinnati, OH 45201
(Unclassified Only)
Olcy Attn ORDAS-L (Tech Lib)

Director
U.S. Army Engr Waterways Exper
Station
P O Box 631
Vicksburg, MS 39180
Olcy Attn WESSD G Jackson
Olcy Attn WESSA W Flathau
Olcy Attn J Strange
Olcy Attn WESSE L Ingram
Olcy Attn Library

Commander
U.S. Army Foreign Science & Tech Ctr
220 7th Street, NE
Charlottesville, VA 22901
Olcy Attn DRXST-SD

Commander
U.S. Army Material & Mechanics
Rsch Ctr
Watertown, MA 02172
(Address CNWDI: Attn:
Document Control for)
Olcy Attn Technical Library
Olcy Attn DRXMR J Mescall
Olcy Attn DRXMR-TE R SHEA

Commander
U.S. Army Material Dev & Readiness
CMD
5001 Eisenhower Avenue
Alexandria, VA 22333
Olcy Attn DRCDE-D L Flynn
Olcy Attn DRXAM-TL (Tech Lib)
Uncl only

Commander
U.S. Army Missile Command
Redstone Arsenal, AL 35809
Olcy Attn DRDMI-XS
Olcy Attn RSIC

Commander
U.S. Army Mobility Equip R&D CMD
Fort Belvoir, MD 22060
(CNWDI to Army Mat Dev
& Readiness Command)
Olcy Attn DRDME-WC (Tech Lib)

Commander
U.S. Army Nuclear & Chemical Agency
7500 Backlick Road
Building 2073
Springfield, VA 22150
(desires only 1cy to Library)
Olcy Attn Library

Deputy of Chief of Staff for
  OPS & Plans
Department of the Army
Washington, DC 20310
    01cy Attn DAMO-NC

Commander
Harry Diamond Laboratories
Department of the Army
2800 Powder Mill Road
Adelphi, MD 20783
    (CNWDI-Inner Envelope:
    Attn: DELHD-RBH)
    01cy Attn Chief Div 20000
    01cy Attn DELHD-I-TL (Tech Lib)

Commander
U.S. Army Armament Material Readiness
  Command
Rock Island, IL 61202
    01cy Attn MA Library

Director
U.S. Army Ballistic Research Labs
Aberdeen Proving Ground, MD 21005
    01cy Attn DRDAR-BLE J Keefer
    02cy Attn DRDAR-TSB-S (Tech Lib)
    01cy Attn DRDAR-BLT W Taylor
    01cy Attn DRDAR-BLV

Commander
U.S. Army Communications Command
Fort Huachuca, AZ 85613
    01cy Attn Technical Reference Div

Commander
U.S. Army Concepts Analysis Agency
8120 Woodmont Avenue
Bethesda, MD 20014
    01cy Attn MOCA-ADL (Tech Lib)

Commander
U.S. Army Engineer Center
Fort Belvoir, VA 22060
    01cy Attn ATZA

Division Engineer
U.S. Army Engineer Div Huntsville
P O Box 1600, West Station
Huntsville, AL 35807
    01cy Attn HNDED-SR

Division Engineer
U.S. Army Engineer Div Ohio River
P O Box 1159
Cincinnati, OH 45201
    (Unclassified Only)
    01cy Attn ORDAS-L (Tech Lib)

Director
U.S. Army Engr Waterways Exper
  Station
P O Box 631
Vicksburg, MS 39180
    01cy Attn WESSD G Jackson
    01cy Attn WESSA W Flathau
    01cy Attn J Strange
    01cy Attn WESSE L Ingram
    01cy Attn Library

Commander
U.S. Army Foreign Science & Tech Ctr
220 7th Street, NE
Charlottesville, VA 22901
    01cy Attn DRXST-SD

Commander
U.S. Army Material & Mechanics
  Rsch Ctr
Watertown, MA 02172
    (Address CNWDI: Attn:
    Document Control for)
    01cy Attn Technical Library
    01cy Attn DRXMR J Mescall
    01cy Attn DRXMR-TE R SHEA

Commander
U.S. Army Material Dev & Readiness
  CMD
5001 Eisenhower Avenue
Alexandria, VA 22333
    01cy Attn DRCDE-D L Flynn
    01cy Attn DRXAM-TL (Tech Lib)
        Uncl only

Commander
U.S. Army Missile Command
Redstone Arsenal, AL 35809
    01cy Attn DRDMI-XS
    01cy Attn RSIC

Commander
U.S. Army Mobility Equip R&D CMD
Fort Belvoir, MD 22060
    (CNWDI to Army Mat Dev
    & Readiness Command)
    01cy Attn DRDME-WC (Tech Lib)

Commander
U.S. Army Nuclear & Chemical Agency
7500 Backlick Road
Building 2073
Springfield, VA 22150
    (desires only 1cy to Library)
    01cy Attn Library

Air Force Geophysics Laboratory
Hanscom AFB, MA 01731
Olcy Attn LWW K Thompson

Air Force Institute of Technology
Air University
Wright-Patterson AFB, OH 45433
(Does not desire classified documents)
Olcy Attn Library

Headquarters
Air Force Systems Command
Andrews AFB
Washington, DC 20334
Olcy Attn DLW

Air Force Waapons Laboratory, AFSC
Kirtland AFB, NM 87117
Olcy Attn NTES-C R Henny
Olcy Attn NTED R Matalucci
Olcy Attn NTE M Plamondon
Olcy Attn R Guice
Olcy Attn SUL W Lee
Olcy Attn DEX

Assistant Chief of Staff
Intelligence
Department of the Air Force
Washington, DC 20330
Olcy Attn IN

Ballistic Missle Office/DE
Air Force Systems Command
Norton AFB, CA 92409
(Civil Engineering)
Olcy Attn DEB

Ballistic Missle Office/MN
Air Force Systems Command
Norton AFB, CA 92409
(Minuteman) MNNX
Olcy Attn MNNXH D Gage

Deputy Chief of Staff
Research, Development, & ACC
Department of the Air Force
Washington, DC 20330
Olcy Attn AFRDQSM

Deputy Chief of Staff
Logistics & Engineering
Department of the Air Force
Washington, DC 20330
Olcy Attn LEEE

Commander
Foreign Technology Division, AFSC
Wright-Patterson AFB, OH 45433
Olcy Attn NIIS Library

Commander
Rome Air Development Center, AFSC
Griffiss AFB, NY 13441
(Desires no CNWDI)
Olcy Attn TSLD

Stragetic Air Command/XPFS
Department of the Air Force
Offutt AFB, NB 68113
Olcy Attn NRI-STINFO Library
Olcy Attn XPFS

Department of Energy
Albuquerque Operations Office
P O Box 5400
Albuquerque, NM 87115
Olcy Attn CTID

Department of Energy
Washington, DC 20545
Olcy Attn OMA/RD&T

Department of Energy
Nevada Operations Office
P O Box 14100
Las Vegas, NV 89114
Olcy Attn Mail & Records for Technical Library

Department of the Interior
Bureau of Mines
Bldg. 20, Denver Federal Ctr
Denver, CO 80225
Olcy Attn Tech Lib (Uncl only)

Director
Federal Emergency Management Agency
1721 I Street, NW
Washington, DC 20472
Olcy Attn Hazard Eval & Vul Red Div

Aerospace Corp.
P O Box 92957
Los Angeles, CA 90009
Olcy Attn H Mirels
Olcy Attn Technical Infor Services

Agbabian Associates
250 N Nash Street
El Segundo, CA 90245
Olcy Attn M Agbabian

Analytic Services, Inc.
400 Army-Navy Drive
Arlington, VA 22202
Olcy Attn G Hesselbacher

Applied Theory, Inc.
1010 Westwood Blvd.
Los Angeles, CA 90024
(2cys if unclass or
1cy if class)
Olcy Attn J Trulio

Artec Associates, Inc.
26046 Eden Landing Road
Hayward, CA 94545
Olcy Attn S Gill

Avco Research & Systems Group
201 Lowell Street
Wilmington, MA 01887
Olcy Attn Library A830

BDM Corp.
7915 Jones Branch Drive
McLean, VA 22102
Olcy Attn A Lavagnino
Olcy Attn T Neighbors
Olcy Attn Corporate Library

BDM Corp.
P O Box 9274
Albuquerque, NM 87119
Olcy Attn R Hensley

Boeing Co.
P O Box 3707
Seattle, WA 98124
Olcy Attn M/S 42/37 R Carlson
Olcy Attn Aerospace Library

California Research & Technology, Inc.
6269 Variel Avenue
Woodland Hills, CA 91364
Olcy Attn Library
Olcy Attn K Kreyenhagen

California Research & Tech, Inc.
4049 First Street
Livermore, CA 94550
Olcy Attn D Orphal

Calspan Corp.
P O Box 400
Buffalo, NY 14225
Olcy Attn Library

Denver, University of
Colorado Seminary
Denver Research Institute
P O Box 10127
Denver, CO 80210
(Only 1cy of class rpts)
Olcu Attn Sec Officer for
J Wisotski

EG&G Washington Analytical
Services Center, Inc.
P O Box 10218
Albuquerque, NM 87114
Olcy Attn Library

Eric H. Wang
Civil Engineering Rsch Fac
University of New Mexico
University Station
P O Box 25
Albuquerque, NM 87131
Olcy Attn N Baum

Gard, Inc.
7449 N Natchez Avenue
Niles, IL 60648
Olcy Attn G Neidhardt
(Uncl only)

General Electric, Co
Space Division
Valley Forge Space Center
P O Box 8555
Philadelphia, PA 19101
Olcy Attn M Bortner

General Electric Co.-Tempo
816 State Street (P O Drawer QQ)
Santa Barbara, CA 93102
Olcy Attn DASIAC

General Research Corp.
Santa Barbara Division
P O Box 6770
Santa Barbara, CA 93111
Olcy Attn B Alexander

Higgins, Auld Association
2601 Wyoming Blvd NE
Albuquerque, NM 87112
Olcy Attn J Bratton

IIT Research Institute
10 W 35th Street
Chicago, IL 60616
Olcy Attn Documents Library
Olcy Attn R Welch
Olcy Attn M Johnson

Information Science, Inc.
123 W Padre Street
Santa Barbara, CA 93105
Olcy Attn W Dudziak

Institute for Defense Analyses
400 Army-Navy Drive
Arlington, VA 22202
Olcy Attn Classified Library

J H Wiggins Co., Inc.
1650 S Pacific Coast Highway
Redondo Beach, CA 90277
Olcy Attn J Collins

Kaman Avidyne
83 Second Street
Northwest Industrial Park
Burlington, MA 01803
Olcy Attn Library
Olcy Attn E Criscione
Olcy Attn N Hobbs
Olcy Attn R Ruetenik

Kaman Sciences Corp.
P O Box 7463
Colorado Springs, CO 80933
Olcy Attn F Shelton
Olcy Attn Library

Kaman Sciences Corp.
Southern California Operations
101 Continental Blvd Suite 855
El Segundo, CA 90245
Olcy Attn D Sachs

Lawrence Livermore National Lab.
P O Box 808
Livermore, CA 94550
Olcy Attn DOC CON for L-200 T Butkovich
Olcy Attn DOC CON for Tech Infor Dept. Library
Olcy Attn DOC CON for L-205 J Hearst (Class L-203)
Olcy Attn DOC CON for L-90 D Norris (Class L-504)
Olcy Attn DOC CON for L-437 R Schock
Olcy Attn DOC CON for L-7 J Kahn
Olcy Attn DOC CON for L-96 L Woodruff (Class L-94)
Olcy Attn DOC CON fro L-90 R Dong

Lockheed Missiles & Space Co., Inc.
P O Box 504
Sunnyvale, CA 94086
Olcy Attn TIC-Library

Los Alamos National Scientific Lab.
Mail Station 5000
P O Box 1663
Los Alamos, NM 87545
Olcy Attn MS 670/J Hopkins
Olcy Attn DOC CON for M Sanpford
Olcy Attn DOC CON for R Whittaker
Olcy Attn DOC CON for MS 364 (Class Reports Lib)
Olcy Attn DOC CON for G Spillman
Olcy Attn DOC CON for A Davis
Olcy Attn DOC CON for R Bridwell

Lovelace Biomedical & Environmental Research Institute, Inc.
P O Box 5890
Albuquerque, NM 87115
Olcy Attn R Jones (Unclas only)

Martin Marietta Corp.
P O Box 5837
Orlando, FL 32855
Olcy Attn G Fotieo

McDonnell Douglas Corp.
5301 Bolsa Avenue
Huntington Beach, CA 92647
Olcy Attn R Halprin

Merritt Cases, Inc.
P O Box 1206
Redlands, CA 92373
Olcy Attn J Merritt
Olcy Attn Library

Meteorology Research, Inc.
464 W Woodbury Road
Altadena, CA 91001
Olcy Attn W Green

Nathan M. Newmark Consult
Eng Services
3106A Civil Eng Bldg.
University of Illinois
Urbana, IL 61801
Olcy Attn N Newmark

Oak Ridge National Lab.
Nuclear Division
Z-10 Lab Records Div
P O Box X
Oak Ridge, TN 37830
Olcy Attn Civil Def Res Proj
Olcy Attn DOC CON for Central Research Library

Pacifica Technology
P O Box 148
Del Mar, CA 92014
Olcy Attn G Kent
Olcy Attn R Bjork

Physics International Co.
2700 Merced Street
San Leandro, CA 94577
Olcy Attn E Moore
Olcy Attn L Behrmann
Olcy Attn Technical Library
Olcy Attn F Sauer

R & D Associates
P O Box 9695
Marina Del Rey, CA 90291
Olcy Attn Technical Infor Ctr
Olcy Attn A Latter
Olcy Attn A Kuhl
Olcy Attn J Carpenter
Olcy Attn C MacDonald
Olcy Attn R Port
Olcy Attn J Lewis

Rand Corp.
1700 Main Street
Santa Monica, CA 90406
Olcy ATTN C Mow

Sandia Laboratories
Livermore Laboratory
P O Box 969
Livermore, CA 94550
Olcy Attn DOC CON for Library & Security Class Division

Sandia National Laboratories
P O Box 5800
Albuquerque, NM 87185
(Attn Mail Services Section for Intended Recipient)
Olcy Attn Mail Ser Sec W Roherty
Olcy Attn Mail Ser Sec 3141
Olcy Attn Mail Ser Sec L Vortman
Olcy Attn Mail Ser Sec A Chaban
Olcy Attn Mail Ser Sec L Hill

Science Applications, Inc.
P O Box 2351
La Jolla, CA 92038
Olcy Attn Technical Library

Science Applications, Inc.
1257 Tasman Drive
Sunnyvale, CA 94086
Olcy Attn J Dishon

Science Applications, Inc.
2450 Washington Avenue
San Leabdro, CA 94577
Olcy Attn D Maxwell
Olcy Attn D Bernstein

Science Applications, Inc.
P O Box 1303
McLean, VA 22102
Olcy Attn M Knasel
Olcy Attn B Chambers III
Olcy Attn R Sievers
Olcy Attn J Cockayne

Southwest Research Institute
P O Drawer 28510
San Antonio, TX 78284
Olcy Attn W Baker
Olcy Attn A Wenzel

SRI International
333 Ravenswood Avenue
Menlo Park, CA 94025
Olcy Attn G Abrahamson

Systems, Science & Software, Inc.
P O Box 1620
La Jolla, CA 92038
Olcy Attn Library
Olcy Attn D Grine
Olcy Attn T Riney
Olcy Attn K Pyatt

Teledyne Brown Engineering
Cummings Research Park
Huntsville, AL 35807
    Olcy Attn J Ravenscraft

Terra Tek, Inc.
420 Wakara Way
Salt Lake City, UT 84108
    Olcy Attn Library
    Olcy Attn S Green
    Olcy Attn A Jones

Tetra Tech, Inc.
630 N Rosemead Blvd.
Pasadena, CA 91107
    Olcy Attn L Hwang
    Olcy Attn Library

TRW Defense & Space Sys Group
One Space Park
Redondo Beach, CA 90278
    Olcy Attn I Alber
    Olcy Attn Tech Infor Ctr
    O2cy Attn N Lipner
    Olcy Attn P Bhutta
    Olcy Attn D Baer
    Olcy Attn R Plebuch

TRW Defense & Space Sys Group
P O Box 1310
San Bernardino, CA 92402
    Olcy Attn E Wong
    Olcy Attn P Dai

Universal Analytics, Inc.
7740 W Manchester Blvd
Playa Del Rey, CA 90291
    Olcy Attn E Field

Weidlinger Assoc., Consulting Eng
110 E 59th Street
New York, NY 10022
    Olcy Attn M Baron

Weidlinger Assoc., Consulting Eng
3000 Sand Hill Road
Menlo Park, CA 94025
    Olcy Attn J Isenberg

Westinghouse Electric Corp.
Marine Division
Hendy Avenue
Sunnyvale, CA 94088
    Olcy Attn W Volz

Code 2628 - 20 copies

D. Book - Code 4040 - 100 copies